Environmental Science & Technology

Critical Review

Cite This: Environ. Sci. Technol. 2019, 53, 10007−10022

pubs.acs.org/est

Aging Effects on Biomass Burning Aerosol Mass and Composition: A Critical Review of Field and Laboratory Studies

Anna L. Hodshire,*[,†] Ali Akherati,[‡] Matthew J. Alvarado,[§] Benjamin Brown-Steiner,[§] Shantanu H. Jathar,[‡] Jose L. Jimenez,[∥] Sonia M. Kreidenweis,[†] Chantelle R. Lonsdale,[§] Timothy B. Onasch,[⊥] Amber M. Ortega,[#,▽] and Jeffrey R. Pierce[†]

[†]Department of Atmospheric Science, Colorado State University, Fort Collins, Colorado 80523, United States

[‡]Department of Mechanical Engineering, Colorado State University, Fort Collins, Colorado 80523, United States

[§]Atmospheric and Environmental Research, Inc., Lexington, Massachusetts 02421, United States

[∥]Dept. of Chemistry and Cooperative Institute for Research in Environmental Sciences (CIRES), University of Colorado, Boulder, Colorado 80309, United States

[⊥]Aerodyne Research Inc., Billerica, Massachusetts 01821, United States

[#]Dept. Atmospheric and Oceanic Sciences Department and Cooperative Institute for Research in Environmental Sciences (CIRES), University of Colorado, Boulder, Colorado 80309, United States

Supporting Information

ABSTRACT: Biomass burning is a major source of atmospheric particulate matter (PM) with impacts on health, climate, and air quality. The particles and vapors within biomass burning plumes undergo chemical and physical aging as they are transported downwind. Field measurements of the evolution of PM with plume age range from net decreases to net increases, with most showing little to no change. In contrast, laboratory studies tend to show significant mass increases on average. On the other hand, similar effects of aging on the average PM composition (e.g., oxygen-to-carbon ratio) are reported for lab and field studies. Currently, there is no consensus on the mechanisms that lead to these observed similarities and differences. This review summarizes available observations of aging-related biomass burning aerosol mass concentrations and composition markers, and discusses four broad hypotheses to explain variability within and between field and laboratory campaigns: (1) variability in emissions and chemistry, (2) differences in dilution/entrainment, (3) losses in chambers and lines, and (4) differences in the timing of the initial measurement, the baseline from which changes are estimated. We conclude with a concise set of research needs for advancing our understanding of the aging of biomass burning aerosol.

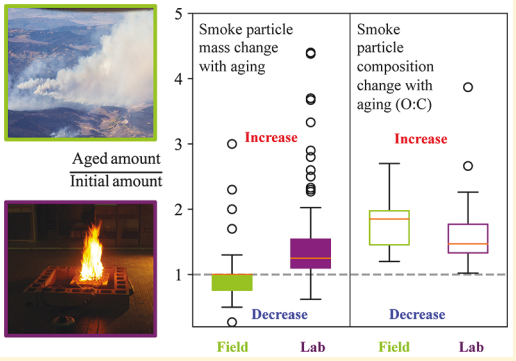

1. INTRODUCTION

Fires have been part of Earth's landscape for over 400 million years,[1] with an estimated annual average of 464 Mha (~3.5% of Earth's ice-free land surface) burning each year between 2001 and 2010.[2] Emissions from biomass burning (BB) provide a major source of primary particles (aerosols) and aerosol precursor vapors to the atmosphere.[3−13] Emissions include primary carbonaceous aerosols (black carbon (BC) and primary organic aerosol, POA;[5−8,14,15]); inorganic aerosol species including potassium, chloride, sulfate, and other inorganic salts and trace minerals;[6,7,16] and inorganic and organic vapors,[4,5,9−13] all of which undergo chemical and physical aging as the plume is transported downwind.[7,17−46] In this review, we focus on BB emissions from the open-air combustion of fuels present in wildfires, prescribed fires (planned fires used for land management), and agricultural burns, and do not include contained combustion of residential biomass fuels and commercial biofuels. We primarily discuss daytime aging, as few studies have thus far explicitly studied nighttime aging of BB emissions.[21,22,47]

Aerosol derived from BB sources contribute to the total ambient particulate matter (PM) concentration,[5−8] with significant implications for climate,[40,48−50] air quality,[51−55] and human health.[56−62] BB smoke aerosols impact the climate directly by absorbing and scattering incoming solar radiation[63,64] and indirectly by acting as cloud condensation and ice nuclei, thereby altering cloud properties.[65−68] Both of these effects depend on the particle size, mass, and composition.[69,70] As the climate warms, North American wildfires have increased

Received: April 29, 2019
Revised: July 24, 2019
Accepted: July 31, 2019
Published: July 31, 2019

DOI: 10.1021/acs.est.9b02588
Environ. Sci. Technol. 2019, 53, 10007−10022

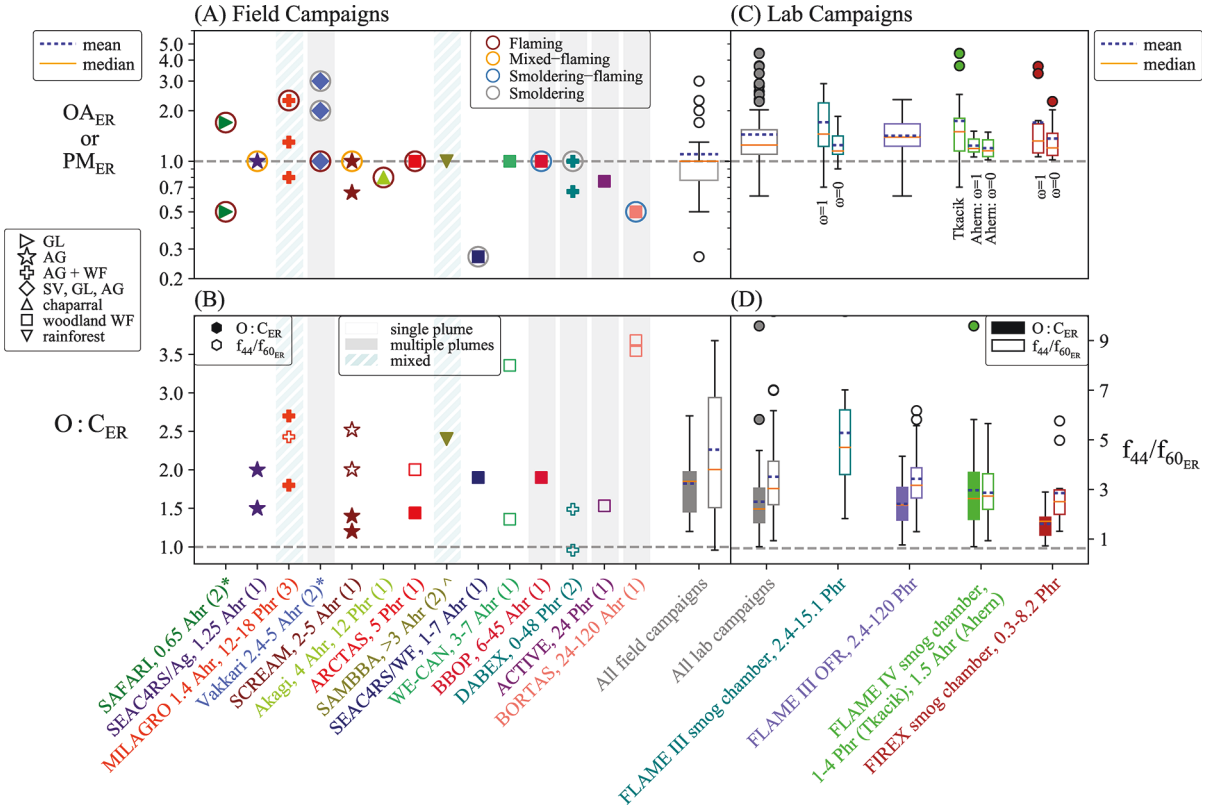

Figure 1. (A) The OA or PM mass enhancement ratio (OA_{ER} or PM_{ER}) and (B) O:C_{ER} (left *y* axis; closed symbols) and $f_{44}/f_{60_{ER}}$ (right *y* axis; open symbols) values for each published field campaign that provides both fresh (within 1 reported hour of emission) and aged measurements. The *x* axis labels indicate campaign or first-author name; final age as actual/physical (A) or photochemical (P); and number of studies associated with a campaign in "()". Photochemical age is the number of hours with an OH exposure of 1.5×10^6 molecules cm^{-3} that equals the same total estimated OH exposure of the field data. Not all studies provide O:C_{ER} and $f_{44}/f_{60_{ER}}$ information. Excluding the SAFARI study (which has two separate estimates from the same plume), multiple points within a study indicate the range of observations. Studies within gray bars indicate that multiple fires/plumes are included in the analyses; studies within gray hatched bars indicate that both multiple fires and a single fire was included in the campaign's analyses; and studies without bars indicate that a single plume was tracked downwind by aircraft. Each symbol indicates the fuel or biome type, as given by the publications. WF = wildfire, SV = savannah, AG = agricultural, GL = grassland. The colored circles around OA_{ER} values indicate burn conditions, where mixed—flaming and smoldering—flaming indicates that a range between mixed and flaming or smoldering to flaming was reported. Burn conditions were reported in each publication by modified combustion efficiency, ΔBC/ΔCO, or visual appearance (SI Table S1). (C) OA_{ER} and (D) O:C_{ER} (left *y* axis; closed symbols or box-and-whisker) and $f_{44}/f_{60_{ER}}$ (right *y* axis; open symbols or box-and-whisker) for each laboratory campaign that has focused on aging. Each box-and-whisker represents all experiments performed within a study. The *x* axis labels indicate campaign name and final photochemical or actual age. The FLAME III OFR data is for the maximum OA_{ER} reported for each burn. The horizontal dashed gray line at 1 in each panel indicates no change from the initial values with age. The whiskers here and in all other box plots extend to the last datum greater than Q1-whisker*IQR and less than Q3+whisker*IQR (IQR = interquartile range, Q3−Q1).

in frequency, intensity, and area[71,72] and are predicted to continue to do so.[73,74] Air quality regulations have successfully decreased $PM_{2.5}$ concentrations (that is, total mass of particles 2.5 μm in diameter and smaller) in the U.S. (EPA, 2018), but these reductions may be offset in the future by $PM_{2.5}$ from increasing BB sources.[62,75,76]

As smoke ages, the mass, composition, and properties of BB vapors and aerosols evolve due to complex competing chemical and physical processes.[7,17−33,35−38,45,77] The vapors and particles are composed of many thousands of different chemical compounds that span a wide range in volatility (vapor pressures), reactivity, and other properties.[78,79] Volatility governs the partitioning of compounds between the gas- and particle-phase[80−82] and is often reported as the effective saturation concentration in $\mu g\ m^{-3}$ (C^*[82]). Organic compounds are grouped into volatility categories:[83] volatile organic compounds (VOCs; $C^* \geq \sim 10^7$), intermediate-volatility organic compounds (IVOCs, $C^* \sim 10^3-10^6$), semivolatile organic compounds (SVOCs, $C^* \sim 10^0-10^2$), low-volatility organic compounds (LVOCs, $C^* \sim 10^{-3}-10^{-1}$), and extremely low-volatility organic compounds (ELVOCs, $C \leq \sim 10^{-4}$). With chemical aging within plumes, the volatility of compounds may decrease, primarily through functionalization or oligomerization reactions, or increase, primarily through fragmentation.[84−87] Gas-phase compounds that decrease in volatility may partition to the particle phase through condensation, creating secondary organic aerosol (SOA) and adding to aerosol mass. Conversely, semivolatile condensed compounds may evaporate upon dilution of the smoke plume, decreasing aerosol mass. These evaporated compounds may act as SOA precursors that can undergo reactions and recondense with continued aging of the plume. Recent work suggests that the time scales for evaporation may vary based on the particle phase state, and evaporation may also be modified by particle-phase and surface reactions.[88,89]

DOI: 10.1021/acs.est.9b02588
Environ. Sci. Technol. 2019, 53, 10007−10022

BB emissions have been extensively studied through field measurements and laboratory experiments to understand the aging of PM mass and composition in BB plumes, as well as to provide bottom-up estimates of BB PM. However, there is significant variability in the observed aging within and between field and laboratory studies. Field campaigns allow for BB plumes to be characterized in natural settings, but are often truncated/limited by uncontrollable and variable field conditions. A number of studies have focused on determining OA evolution by following plumes downwind to track changes in the gas- and particle-phase as a plume ages.[8,17,19,24,26−29,32−34,45,77,90] Aircraft observations tend to be the dominant measurement platform for characterizing aging plumes, as aircraft can track plumes in a pseudo-Lagrangian manner. Some ground sites have also provided information on plumes that have aged between hours and days.[21−23,25,31] BB laboratory studies have been generally focused on characterizing emissions and simulating atmospheric chemical aging under controlled conditions (e.g., fixed fuel/dilution ratios, controlled oxidants).

Laboratory studies provide control over the environmental and chemical conditions, and can be used to examine the effect of changing one variable at a time, but face challenges in recreating the atmospheric conditions of plumes in the field.

Top-down estimates of BB PM also exist that compare models with bottom up inventories to satellite-based and in situ measurements, and a low-bias of the model could be indicative of BB SOA.[91−94] However, these discrepancies are dominated by uncertainties in the emissions inventories,[95] which is beyond the scope of this paper.

To date, there are significant knowledge gaps that limit a full understanding of how field and laboratory observations can be reconciled. A more complete understanding of the underlying physics and chemistry could explain the observed variability in the evolution of BB mass and composition in field and laboratory experiments. The purpose of this critical review is to provide an overview of observed changes in PM mass and composition markers in field and laboratory studies (Section 2), present possible hypotheses for differences between observations (Section 3), and present research needs for creating a unified framework on BB aerosol aging (Section 4).

2. OVERVIEW OF OBSERVATIONS

2.1. Field Studies. Figure 1A shows whether OA or PM mass was observed to increase or decrease with age in field campaigns. Specifically, ratios of final to initial values of normalized BB aerosol mass are expressed as the mass enhancement ratio (ER),

$$\mathrm{OA_{ER}} = \frac{\Delta\mathrm{OA}/\Delta\mathrm{CO}(f)}{\Delta\mathrm{OA}/\Delta\mathrm{CO}(i)} \quad (1)$$

(where PM replaces OA in eq 1 for PM mass enhancements) for published field campaigns on BB aerosol aging. Δ indicates the difference between the in-plume and background value of OA and CO (i.e., the enhancement of these species concentrations due to BB), f indicates the final available measurement, and i indicates the first (initial) available measurement. Values greater than 1 indicate a net increase in dilution-corrected OA or PM concentrations with aging and values less than 1 indicate a net decrease. CO is used in BB studies as an inert tracer for these short-term (hours to a few days) aging studies to correct for dilution effects, as it has an atmospheric lifetime on the order of 2 months[70] with negligible impacts from chemical production.[96]

Figure 1A only includes studies that have both fresh (within 1 h of emission) and aged measurements, and is sequentially arranged by the final age from youngest (leftmost) to oldest (rightmost). All studies in Figure 1A provide ΔOA/ΔCO from aerosol mass spectrometer (AMS) instruments except the SAFARI observations detailed in Hobbs et al.[32] and the Vakkari et al.[21,22] studies (see Supporting Information (SI)). AMS sensitivities (collection and relative ion efficiencies) have been shown in some studies to vary with organic oxidation levels (see SI), but these issues are unlikely to explain differences between lab and field measurements.

SAFARI[32,97] and the Vakkari studies[21,22] reported total excess particulate matter (TPM) and PM_1; all other studies reported OA.

The two published reports from SAMMBA on BB aerosol aging (one ground-based[23] and one aircraft-based[77]) both report no net OA_{ER}

Across field campaigns (Figure 1A), the OA_{ER} (or PM_{ER}) observations range from increases to no change to decreases in mass with age, with the median, mean, and interquartile ranges (IQR) OA_{ER} values at 1, 1.1, and 0.77−1.0, respectively. These values are much lower than for urban pollution, where $OA_{ER} \sim 5-10$ are often observed with aging, in part due to much smaller urban POA emissions relative to CO and SOA precursors.[98,99] The primary observable trend in mass across the campaigns is that, in the few cases where increases in mass were observed, they occurred at shorter transport ages, with the oldest observation of a net increase in mass from Vakkari et al.,[22] at up to 5 h old. However, it is unclear if this trend is real due to a relatively low number of data points along with variability in fuels, burn conditions, and initial times. No trend is observed when comparing the age of the earliest measurement (ranging from <10−60 min; SI Table S1) to OA_{ER}.

Figure 1B focuses on OA composition, providing enhancement ratios of oxygen-to-carbon, $O{:}C_{ER}$,

$$\mathrm{O{:}\,C_{ER}} = \frac{\mathrm{O{:}\,C}(f)}{\mathrm{O{:}\,C}(i)} \quad (2)$$

and the enhancement ratios of f_{44}/f_{60}, $f_{44}/f_{60_{ER}}$,

$$f_{44}/f_{60_{ER}} = \frac{f_{44}/f_{60}(f)}{f_{44}/f_{60}(i)} \quad (3)$$

from AMS observations, when available. An elevated fraction of the AMS OA spectra at m/z 60, f_{60}, from the fragmentation of "levoglucosan-like" species (levoglucosan and other molecules that similarly fragment in the AMS[26,100,101]) has been shown to be a tracer of BB.[26] Although f_{60} decreases under photochemical aging,[102,103] it can still remain present at levels above background on aging time scales of at least 1 day.[26] Mass fraction f_{44} can be used as a surrogate for SOA[104−106] with relative increases in f_{44} indicative of more oxidized OA.[107] In recent years, f_{44}/f_{60} has been used to qualitatively explore the amount of oxidative processing of particles in BB plumes.[26,29,34] AMS measurements also provide the total elemental oxygen and carbon content of the measured aerosol, with the atomic oxygen/carbon ratio (O:C) shown to be linearly correlated with f_{44} in OA.[108,109] Thus, increases in either or both of f_{44}/f_{60} and O:C indicate BB OA aging.

Unlike OA_{ER}, all observations except one of composition increase in $O{:}C_{ER}$ and $f_{44}/f_{60_{ER}}$ (Figure 1B). The median and

DOI: 10.1021/acs.est.9b02588
Environ. Sci. Technol. 2019, 53, 10007−10022

IQR O:C_{ER} values lie at 1.85 and 1.5−2.0; the median and IQR $f_{44}/f_{60_{ER}}$ values lie at 3.8 and 2.3−6.7. This increase indicates that particles are almost always becoming more oxidized even if OA_{ER} decreases with age. These values are similar to urban environments, where the O:C_{ER} would be 1.2−2.1 for 6−48 h of photochemical aging.[110] However, the balance of chemical and physical processes affecting OA aging may differ between urban and BB systems.

The field campaigns in Figure 1A,B fall into two general study designs: either a single smoke plume is sampled by aircraft as it travels downwind or multiple plumes are characterized both at and near the fires' sources. In the latter design, characterization of smoke transported downwind from these fire becomes more complex. In many of these aggregate (multiple plume) cases, the smoke characterized downwind was unlikely to be the same smoke that was sampled near the source, which introduces irreducible uncertainty into plume intercomparisons.[21−24,34,111] No clear trend for mass or composition appears between the single plume and aggregate studies.

We have attempted to categorize fires by fuel type and burn conditions (e.g., flaming, smoldering, or both) in Figure 1A,B, based on information in existing publications. Burn conditions are often estimated using (1) the modified combustion efficiency (MCE = $\Delta CO_2/(\Delta CO+CO_2)$[112]), (2) the ratio of excess BC to CO, $\Delta BC/\Delta CO$,[7] or (3) the visual appearance of the fire. We use an MCE cutoff of 0.9, with MCE > 0.9 indicating more flaming, MCE < 0.9 indicating more smoldering, and MCE around 0.9 indicating a mixture of flaming and smoldering conditions.[5] Three studies use $\Delta BC/\Delta CO$ to classify the burn conditions and we follow their classifications.[7,21,22] The implications of the burn conditions and fuel types are discussed in Section 3.1.

The findings from the field campaigns evident in Figure 1A, B are

- OA_{ER} and PM_{ER} observations show variability, with median and mean changes of 1.0 and 1.1, respectively. All cases with increases in mass occurred at shorter transport ages (<5 h). These ratios are much lower than that for urban pollution.
- All studies investigating OA composition markers showed increased oxidation with aging (increasing O:C_{ER} and $f_{44}/f_{60_{ER}}$).

2.2. Laboratory Studies. Figure 1C,D details the aggregate OA_{ER}, O:C_{ER}, and $f_{44}/f_{60_{ER}}$ for each campaign as box-and-whisker plots (SI Figure S1 provides the same information for all individual burns). Figure 1C,D includes results from three studies at the U.S. Forest Service Fire Science Laboratory (FSL) in Missoula, MT, with specific focus on BB aging: FLAME III, FLAME IV, and FIREX. These campaigns provided data from 22 fuel types and eight different oxidation methods across 84 experiments.[113−116] FLAME III, FLAME IV, and FIREX analyzed aging of smoke in Teflon environmental ("smog") chambers.[113,115,116] FLAME III also performed aging experiments in an oxidation flow reactor (OFR).[114] The residence times within the smog chambers range between 1 and 6 h, with photochemical ages between 0.3 and 25 equiv hours (assuming OH = 1.5×10^6 molec. cm^{-3} for all studies except Tkacik et al.[115] which assumed OH = 2×10^6 molec. cm^{-3} and 60 ppb of O_3; Figure 1 and SI Figure S2). The OFR had a residence time of 180 s, with maximum OA_{ER} values observed at 40−105.6 h (Figure 1 and SI Figure S2). Further details can be found in the SI.

The laboratory OA_{ER} values in Figure 1C are mostly >1. The range of values in the smog-chamber experiments depend on the assumptions used to correct for particle wall losses (PWL; details on each study's PWL methods are included in the SI). Vapors can either partition with aerosol that have deposited on the chamber walls ("ω = 1" case[117]) or only partition to suspended particles ("ω = 0" case[117]). Figure 1C shows both box-and-whiskers for both the ω = 1 and ω = 0 cases from the Hennigan et al.[113] Ahern et al.,[116] and FIREX analyses (Tkacik et al.[115] only provided the ω = 1 case). As expected, the ω = 0 case yields a slightly lower mass enhancement. For FLAME IV, Ahern et al.[116] included six fewer experiments than Tkacik et al.[115] and used different final times (eq 1), so caution should be taken when directly comparing OA_{ER} between the two studies. None of the data presented were corrected for vapor wall losses, which is important for determining OA_{ER} in smog chamber studies,[118,119] and is discussed in Section 3.3. As the residence time is short in the OFR and particle losses are measured to be small, Ortega et al.[114] instead reports OA_{ER} without correcting for potential wall losses.

Despite the variation in both physical and photochemical ages (Figure 1 and SI Figure S2) and PWL correction methods between the campaigns, the median, mean, and IQR OA_{ER} values are generally similar. The median and mean mass enhancements range between 1.15 and 1.45 and 1.2−1.74, respectively, and the IQRs range between 1.07 and 2.23 (Figures 1C). The median and mean OA_{ER} for all reported laboratory data are 1.25 and 1.44, 25% and 30% higher than the median and mean mass enhancements observed for all reported field data. Further, the IQR for the field data is 0.76−1.3 and 1.1−1.54 for the laboratory data, indicating that the laboratory data are consistently higher in mass enhancement than the field data. A two-sided Mann−Whitney U test on the means between the field and laboratory OA_{ER} data shows the means were significantly different with a p-value of 5×10^{-5}.

In contrast to the mass enhancement observations, the range in the reported O:C_{ER} and $f_{44}/f_{60_{ER}}$ laboratory data are consistent with the field data in the direction and magnitude of change with aging. The median and IQR O:C_{ER} across all laboratory data are 1.5 and 1.3−1.8, and the median and IQR for $f_{44}/f_{60_{ER}}$ across all laboratory data are 3.0 and 1.8−3.6. Sampled plumes in the field undergo, on average, slightly more compositional aging than the emissions in the laboratory aging studies, although the number of data points for the field data is small ($N \leq 10$). The FLAME III data show a higher $f_{44}/f_{60_{ER}}$ mean and median than the field data, potentially due to this study's AMS detecting fragments other than those from CO_2^+.[114]

The findings from the laboratory campaigns evident in Figure 1C, D are

- OA_{ER} in laboratory observations tends to increase under aging, with a median and mean OA_{ER} of 1.4 and 1.7.
- OA_{ER} values in smog-chamber experiments are sensitive to PWL correction methods.
- All studies show chemical signs of aging (increasing O:C_{ER} and $f_{44}/f_{60_{ER}}$), overlapping the range of the field data.

2.3. Variability between Field and Laboratory Campaigns Limits the Community from Creating a

DOI: 10.1021/acs.est.9b02588
Environ. Sci. Technol. 2019, 53, 10007−10022

Unified Framework for BB Aging. When comparing OA_{ER}, $O:C_{ER}$, and $f_{44}/f_{60_{ER}}$ between field and laboratory data (Figure 1), the broad points are as follows:

- On average, laboratory observations show increases in mass with age (OA_{ER} that are mostly >1), whereas on average the field data undergo no net change in mass with age ($OA_{ER} \sim 1$).
- Across all studies, $O:C_{ER}$ and $f_{44}/f_{60_{ER}}$ increase with age, with field observations showing on average a slightly greater increase in $O:C_{ER}$ and $f_{44}/f_{60_{ER}}$.

The variability within and between field and laboratory studies currently prevents the community from creating a unified framework for predicting the aging of BB aerosol. Given the magnitude of the global BB POA source,[26] this results in a significant uncertainty in the global OA budgets.

3. HYPOTHESES FOR VARIABILITY WITHIN AND BETWEEN LAB AND FIELD OBSERVATIONS

In this section, we present four broad categories of hypotheses for the observed variability in OA aging within and between lab and field observations: (1) variability in emissions and chemistry; (2) differences in dilution rates, partitioning, and absolute OA loading; (3) line and chamber wall losses; and (4) differences in the timing of the initial measurement.

3.1. Variability in Emissions and Chemistry. Much of the focus in BB aging studies has been on how emissions and chemistry vary between fuels/biomes and burn conditions.[22,32,113−116,120] Hence, we present this as our starting hypothesis for variability in OA aging: variations in emissions and chemistry could explain much of the variability between field and laboratory measurements.

Differences in Fuel Mixtures Lead to Differences in Emissions. Differences in fuel mixtures and conditions (e.g., fuel-moisture content) can lead to differing emissions of gas- and particle-phase species between different burns, leading to potential differences in initial distributions of mass across volatility bins and composition markers. Emission factors (EFs) from BB for a given gas or aerosol species can vary by more than an order of magnitude across different biomasses.[5,121,122] Selimovic et al.[123] found that laboratory burns of both individual and grouped fuels were in reasonable agreement with field data for select trace gases, although this study has limited PM and VOC measurements and more field-to-lab emissions comparisons are required. Emissions vary with time,[29] but the impact of this variability on mass and composition has not yet been well-characterized.

Modeling studies suggest that known SOA precursors like aromatics and terpenes are not sufficient to explain SOA formation in BB plumes.[18,97,114,124] Intensive efforts have been made during the FIREX and FLAME IV campaigns to carefully characterize previously unspeciated and often unmeasured SOA-precursor emissions,[9−13,125−127] and studies are now beginning to connect these species to BB SOA formation.[116]

The studies in Figure 1A are classified by biome and/or fire type based on the published descriptions. It is difficult to determine any trend across the fuel types given the small number of samples. Although all woodland wildfire samples show either no change or a decrease in mass enhancement with age, these aged samples are all over 5 photochemical hours old, the cutoff at which no mass gains are observed within the available data. In addition, there are many important fire-prone biomes not represented within the current studies, such as peatlands and moorlands.[128,129] SI Figure S3 arranges Figure 1A and B by geographic region. The U.S. and boreal North American studies all show no change or decreases in OAER with aging; no other apparent trends are evident. The published BB aging field studies thus far are primarily in North America, with few studies in Africa, Australia, and South America, and no studies in Europe or Asia.

Across the 84 experiments and 161 estimated OA_{ER} values, only 10 OA_{ER} values decrease and all but two of the available $O:C_{ER}$ and $f_{44}/f_{60_{ER}}$ values show net increases (SI Figure S1). However, interstudy differences make it difficult to draw conclusions for fuel types. Different fuel and oxidant combinations were used within each experiment, and almost all experiments show variable OA_{ER}, $O:C_{ER}$, and $f_{44}/f_{60_{ER}}$ within a given fuel type, even within the same study and oxidation method. This variability could come from variable burn conditions (discussed below).

A limited number of fuel-specific comparisons can be made between the laboratory and field studies. The dominant fuel in the Akagi et al.[17] field study, chaparral, was examined in the OFR and CSU smog chamber experiments. The chaparral laboratory burns observe positive mass enhancements, whereas Akagi et al.[17] observes a negative mass enhancement. Similarly, the woodland forest fire studies likely contained mixtures of different pine species and may be compared to the laboratory burns of black spruce, ponderosa pine, lodgepole pine, white spruce, douglas fir, subalpine fir, and engelmann spruce. Two of the field studies show no change,[25,26] three show decreases in mass ratios,[27,33,34] and the majority of laboratory experiments of the listed pine fuels show net increases in OA. It is more than likely that other laboratory-studied fuels were present in many of the field burns; however, due to lack of specific information, we cannot analyze this topic further. As well, POA EFs and/or initial OA/CO are highly variable, even for a given fuel type within lab and field burns (as previous reviews have synthesized; Andrease and Merlet, 2001; Akagi et al., 2011), which adds to the challenge of comparing OA aging across field and lab studies.

Burn Conditions Influence Emissions, And There May Be Key Differences between Field and Laboratory Conditions. Burn conditions (e.g., flaming, smoldering) also influence emissions and aerosol mass, as VOC emissions can decrease with increased flaming combustion.[120,130] SOA precursor emissions may similarly decrease with increased flaming combustion; however, some SOA precursors vary with high- and low-temperature pyrolysis factors instead of directly with MCE.[127] In the field, burn conditions will change both temporally and spatially over time,[127] potentially resulting in changing emissions, and aircraft studies that track a single plume in a semi-Lagrangian sense are unlikely to sufficiently sample a plume with changing burning conditions. Of the 15 field studies that reported burn conditions (Figure 1A, SI Table S1), the majority report flaming to mixed average conditions. For the BORTAS campaign, Jolleys et al.[34] caution that the fresh smoke appeared to be coming from more smoldering conditions but that the aged smoke appeared to be coming from more flaming conditions. Vakkari et al.[22] found that over a 5-year period, observations from the most flaming conditions did not undergo any mass enhancement, whereas the remaining observations increased PM_{ER} in normalized mass with age. Except for Vakkari et al.,[22] there appears to be no

DOI: 10.1021/acs.est.9b02588
Environ. Sci. Technol. 2019, 53, 10007−10022

pattern between flaming, smoldering, and mixed for net mass changes. Similarly, the relative differences in $O:C_{ER}$ and $f_{44}/f_{60_{ER}}$ between studies do not appear to systematically depend on burn conditions.

All but three of the laboratory aging studies that have reported MCE have been for more flaming fires (MCE > 0.9; SI Figure S4). Laboratory studies of the aging of open-air BB aerosol emissions is currently a small subset of the work done to quantify the primary emission factors (EF) of BB aerosol emissions and within the context of the primary EF work, it is still an open question as to how well laboratory burns represent field variability. Some species, such as BC, appear to correlate well between laboratory and field for primary EF measurements.[29] POA emissions from laboratory work exhibit wide and not fully explained variability for a given fuel type and combustion condition. These laboratory measurements of POA can also differ when compared with field observations. One of the drivers underlying the observed discrepancies in POA emissions between laboratory and field measurements may be variable combustion conditions driven by flame propagation through the fuel and the availability of oxygen due to the level of turbulent mixing.[131] Combustion conditions are typically defined by an average MCE but are governed in part by wind, fuel density, and flame dynamics,[132] which may be important factors when comparing laboratory and field measurements.[120] Other important factors between laboratory and field measurements that influence burn conditions include differences in fuel moisture content,[29,120] mixtures of fuel types,[123] and fractions of these fuels that burn in the laboratory relative to the field.[133,134]

Sekimoto et al.[127] identified two distinct high- and low-temperature pyrolysis emission profiles of VOCs that explained on average 85% of the VOC emissions for 15 fuel types. The high- and low- temperature profiles do not correspond exactly to the more commonly used flaming and smoldering categories, and require further study to determine how these temperature-based profiles may aid in predicting both POA and SOA formation, as well as how the different temperature regimes may be identified in field burns. These differences in VOC profiles for the two pyrolysis regimes may help explain why some given fuels show variability in OA_{ER} between experiments even for the same oxidant and campaign.

Oxidant Concentrations Influence Chemistry. In-plume reactions and oxidant concentrations can influence the aerosol mass and composition markers. Higher oxidant concentrations lead to increased rates of reactions that could both functionalize and fragment gas-phase molecules, and enhance heterogeneous chemistry. Functionalization tends to lead to vapors with lower volatilities that can partition to the particle phase, but fragmentation and heterogeneous reactions tend to lead to higher-volatility products that will remain in or enter the gas phase.[84,135,136] Three studies in Figure 1A explicitly attempt to account for the in-plume OH concentration: Hobbs et al.[32] and Yokelson et al.[7] report OH concentrations $>10^7$ molecules cm^{-3} (typical daily averaged ambient tropospheric OH concentrations are $\sim 1.5 \times 10^6$ molecules cm^{-3}), and both of these plumes see a positive mass enhancement (assuming that the analyses of Alvarado and Prinn[97] are correct). Akagi et al.[17] report a slightly elevated in-plume OH concentration of 5.27×10^6 molecules cm^{-3} and observe a net decrease in mass. However, each of these fires were for different environments, fuels, and burn conditions. Without corresponding knowledge of what the ratios of functionalization to fragmentation were, no conclusions can be drawn as to how the enhanced OH concentrations influenced the plumes' PM masses.

Plume oxidant levels can be influenced by NO_x emissions (and thus combustion phase), solar zenith angle, optical depth, temperature, and absolute humidity. The rates of oxidation of VOCs and the resulting production of O_3 in BB plumes is NO_x-limited (Jaffe and Wigder, 2013), and fires with higher NO_x emissions have higher oxidant levels and more active oxidation of VOCs. NO_x emissions depend on the fuel N content as well as the combustion phase, leading to more rapid oxidation in grassland and savannah fires (mainly flaming combustion) than in boreal fires (low fuel N content and more smoldering combustion[137,138]). The solar zenith angle influences the sun's intensity, and the optical depth controls how far sunlight may penetrate the plume, impacting photolysis rates and oxidant concentrations. Temperature controls rates of chemical reactions, with plumes in colder environments (e.g., plumes that reach the free troposphere) likely undergoing slower reactions. Humidity determines the fraction of OH production from O_3 photolysis. However, these factors have not been explicitly accounted for in field or laboratory campaigns.

The Roles of Multiphase and Nighttime Chemistry Are Under-Characterized. The importance of multiphase/condensed-phase reactions and nighttime chemistry (when the nitrate radical can be the most important oxidant[139]) is currently unclear. Multiphase reactions have not yet been explicitly characterized in aging BB studies, although observations of tarball formation may be indicative of heterogeneous chemistry.[140,141] Vakkari et al.[22] observed no net increase in total PM_1 mass concentrations at nighttime but did see net increases in aged mass during daytime conditions (excluding the most flaming fires, as discussed below). Wildfire plumes in the northwest U.S. transported primarily at night versus day showed little difference in mass enhancement.[31] Zhou et al.[31] also find that the OA from plumes transported at night appeared to be less oxidized than the daytime plumes, with daytime $O:C_{ER}$ values higher than nighttime $O:C_{ER}$ values. None of the laboratory data in our review include experiments where the nitrate radical is the primary oxidant, although we do include experiments with dark O_3 chemistry (O_3 is added but UV lights are off) (SI Figure S1). These "Dark O_3" experiments generally do not give higher OA_{ER} values than experiments with UV lights, and hence they are likely not a cause of the relatively high bias in OA_{ER} relative to field experiments.

3.2. Differences in Dilution Rates, Partitioning, and Absolute OA Loading. SVOCs can make up between ~20 and 90% of fresh BB particles,[29,102,142−144] and upon dilution, they may evaporate. Evaporated POA can act as precursor vapors for SOA if they react and form lower-volatility products,[119,145] and the resultant SOA is likely to have a more-aged signal (higher $O:C_{ER}$ and $f_{44}/f_{60_{ER}}$) than the original POA compounds, even if OA_{ER} does not change (POA evaporation could be balanced by recondensation of oxidation products). However, the rate and yield at which evaporated POA forms SOA is uncertain[146] and has not been yet studied for smoke plumes.

As partitioning and evaporation rates depend on absolute aerosol mass loading,[82,147] the initial OA concentration, dilution rate, and concentration of OA in the entrained

DOI: 10.1021/acs.est.9b02588
Environ. Sci. Technol. 2019, 53, 10007−10022

background air will impact OA aging.[145] In addition, the partitioning of semivolatile OA is temperature dependent, with an order of magnitude shift in C* for every 20 K change in temperature.[82] As dilution proceeds differently within and between laboratory and field studies, dilution differences could help explain variability in OA_{ER}, $O{:}C_{ER}$, and $f_{44}/f_{60_{ER}}$. Evaporation is also influenced by oligomerization reactions and the bulk diffusion coefficient. Oligomerization reactions create lower-volatility products,[148] decreasing evaporation rates. Similarly, a decreased particle-phase diffusion coefficient leads to decreased evaporation rates.[88] Oligomerization reactions and the diffusion coefficient for BB aerosol are currently not well-studied, although tar ball formation in BB plumes may indicate both oligomerization processes and a low particle-phase diffusion coefficient.[141]

Field Burns Undergo Variable Dilution Rates. In the field, dilution is influenced by the size of the fire, atmospheric conditions (e.g., stability of the layer of smoke injection), and regional topography. Figure 2 provides the range and distribution of fire sizes for the U.S. for 2014, indicating the importance of small (<0.1 km^2 of burned area) fires. Well over half of the globe's landmass experiences average fire sizes ≤1 km^2.[149] Plumes that dilute quickly, either due to being formed by small fires and/or being dispersed quickly due to atmospheric conditions, will lose more mass to evaporation, all other conditions being equal. Conversely, plumes that dilute slowly, either due to being formed by large fires and/or being dispersed slowly due to atmospheric conditions or regional topography, may lose less mass to evaporation.[119,145] Slowly diluting plumes may also undergo fewer chemical reactions if the plume is dense enough to limit sunlight to the interior of the plume, slowing photochemistry.[32,150,151] Thus, mass and composition markers may change slowly in large plumes if little mass is lost by evaporation or gained from chemistry. However, scattered light from smoke aerosols may compensate for light lost by aerosol absorption.[152]

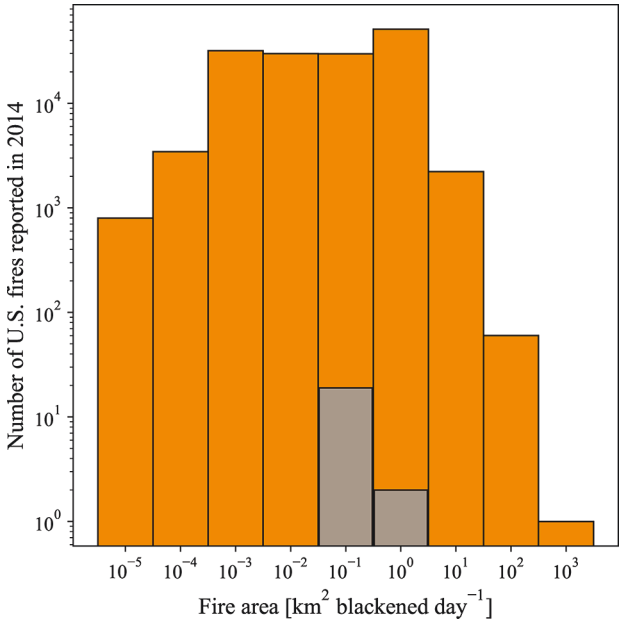

Figure 2. Annual data for the United States in 2014 for the number of recorded fires by fire size in km^2 blackened per day (that is, the total area in km^2 burned per day) from the National Emissions Inventory (U.S. EPA NEI, 2014). Overlain in gray are the number of fires by size from the field campaigns in Figure 1A for each fire with sizes either explicitly reported or estimated within the publication. Note that some campaigns in Figure 1 are not included as this information was not provided, and they typically tended to be larger fires. Adapted from Hodshire et al.[145]

Five of the field studies in Figure 1 explicitly characterized the fire size (Figure 2; SI Table S1, between 0.01 and 10 km^2), and all showed no change or decreases in mass with age. The five woodland wildfires[25−27,33,34] were likely larger than 10 km^2 but also show no change or decreases in mass with age. As mentioned above, there are differences in study design for field campaigns between aircraft studies and ground-based studies, as well as if the aircraft study is explicitly tracking one plume downwind or instead measuring smoke within a region. These differences in measurement design may impact the apparent influence of dilution and is a source of uncertainty.

Laboratory Studies Do Not Undergo Variable Dilution Rates. Unlike field campaigns, laboratory campaigns keep chambers at an effectively fixed dilution ratio. Most laboratory smog-chamber experiments initially dilute OA concentrations to 10−100 $\mu g\ m^{-3}$, and the concentrations generally stay in this range throughout the aging experiment. Hence, smog-chamber and OFR experiments do not sample continuous dilution with time, which may control evaporation and the availability of SOA precursors.

Initial POA Concentrations Influence SOA Production. The FLAME III OFR introduced significantly higher initial OA concentrations into its chamber compared to the three smog chamber experiments, impacting mass. Figure 3 shows OA_{ER} versus the initial OA concentration for all experiments, with SI Figure S5 showing the same for $O{:}C_{ER}$ and $f_{44}/f_{60_{ER}}$. The three smog chambers introduce between ∼5 and 400 $\mu g\ m^{-3}$ of OA, and the OFR introduces between ∼110 and 18 000 $\mu g\ m^{-3}$ of POA. For the OFR, there is a decreasing trend of OA_{ER} with increasing initial OA (R^2 = 0.62). Ortega et al.[114] hypothesized that increasing initial OA concentrations drives more SVOCs (and potentially even IVOCs) to the particle phase, leading to fewer gas-phase SOA precursors available to react and condense onto the particles. A significant amount of mass exists in the C* = 10^3−10^4 $\mu g\ m^{-3}$ range.[12,119] These species are POA at high organic mass concentrations but gas-phase SOA precursors at low organic mass concentrations.[12,82] The smog chambers in Figure 3 are dilute enough that species with C* = 10^3−10^4 $\mu g\ m^{-3}$ range are mostly in the gas phase for all experiments, so additional dilution (lower POA concentrations) does not result in a strong trend in OA_{ER}: Tkacik et al.[115] has an R^2 value of 0.47, and the remaining campaigns have R^2 < 0.25. The OFR $O{:}C_{ER}$ and $f_{44}/f_{60_{ER}}$ data have an inverse correlation to POA with R^2 values of 0.42 and 0.3, respectively. This inverse correlation indicates less condensation of oxidized organics at higher POA loadings, supporting the hypothesis that higher POA loadings reduce OA aging and enhancement.

Figure 3 also includes the field campaigns that provided initial in-plume absolute OA. Many of these field studies provided mass time series, and here we qualify the initial OA as the highest observed OA concentration. In general, the field OA_{ER} are close to 1 for low initial OA loadings (∼<100 $\mu g\ m^{-3}$). However, the field observations with higher initial OA loadings generally have lower OA_{ER} values compared to the trend for the FLAME III OFR. This low field bias is potentially

DOI: 10.1021/acs.est.9b02588
Environ. Sci. Technol. 2019, 53, 10007−10022

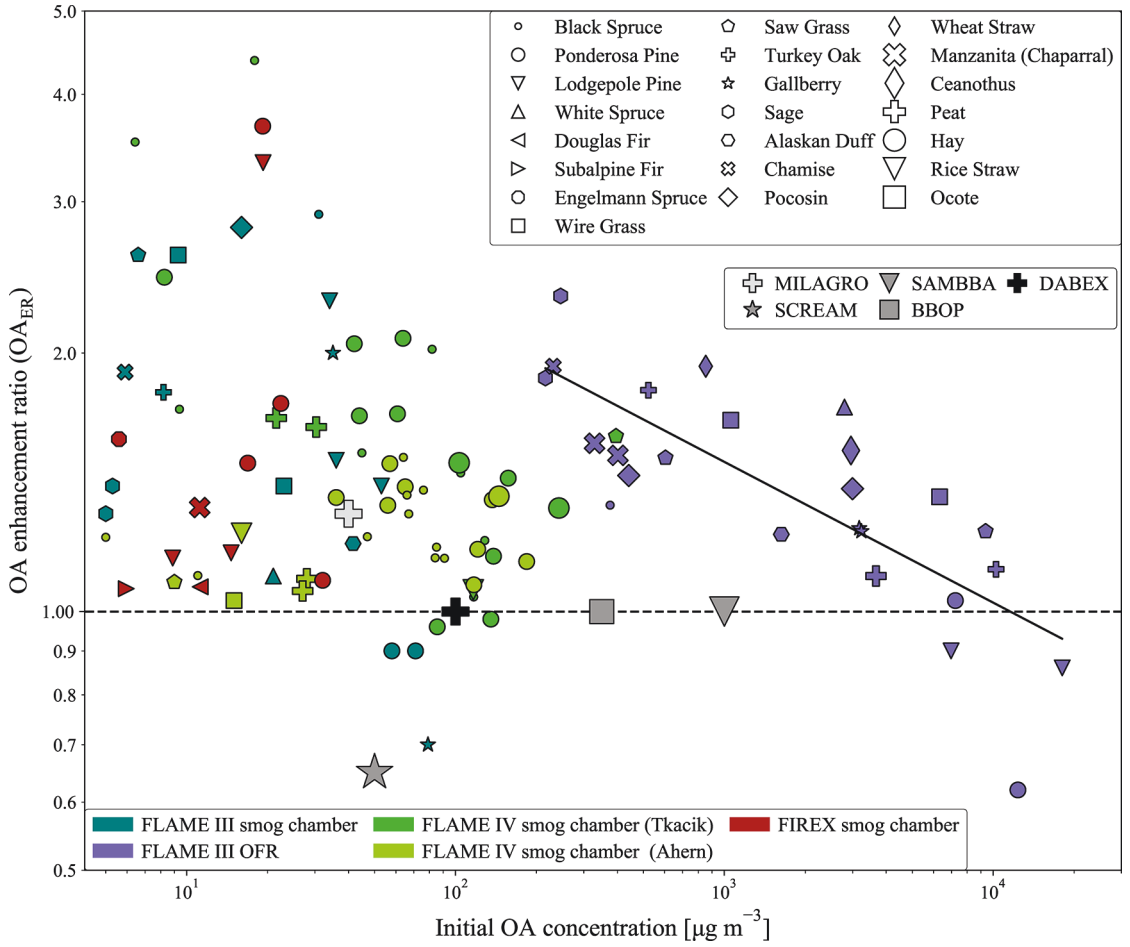

Figure 3. OA enhancement ratio (OA_{ER}) to the initial OA concentration in $\mu g\ m^{-3}$ within each chamber for all experiments within the laboratory campaigns of Figure 1C and D. Symbols indicate fuel type and colors indicate study type. The horizontal dashed black line at $OA_{ER} = 1$ indicates no net change in OA mass from the initial mass. The black solid line indicates the trend line for the OFR data, with a slope of −0.16 and an R^2 value of 0.62. Also included on this figure are the studies that report initial OA concentrations. Where field campaigns published time series of OA, we used the highest concentrations as this is likely the closest overpass over a plume.

because the observed ambient plumes diluted between the initial and final observations while the OA concentrations in the OFR are held approximately fixed during aging.

Background OA Differs between Field Studies. Hodshire et al.[145] indicated that elevated (>20 $\mu g\ m^{-3}$) background aerosol concentrations can impact SOA formation in plumes from smaller fires (<10 km^2), as entrainment of the elevated background aerosol mass can slow evaporation of semivolatile compounds, effectively slowing evaporation caused by dilution. None of the studies in Figure 1A explicitly report the background aerosol concentration (although this information likely is available within the campaign data repositories). This background OA effect could be particularly important in regions that experience large numbers of small fires, such as the Amazon basin during the dry season.[38,153] SI Figure S6 shows that for the U.S. in 2014, 3% of total reported fires occurred in background $PM_{2.5}$ concentrations of ≥20 $\mu g\ m^{-3}$, accounting for 7% of total $PM_{2.5}$ fire emissions. No study to date has explicitly considered the effects on OA_{ER}, $O{:}C_{ER}$, or $f_{44}/f_{60_{ER}}$ from plume size, dilution rates, mixing, and background aerosol and vapor concentrations with ambient data.

Temperature Differs between Field and Laboratory Studies. Temperatures at the height of plume injection may be significantly colder than those at the surface, and these temperature differences could lead to different OA partitioning and aging for plumes at different heights/temperatures. In laboratory experiments, temperature is generally held fixed, and there is currently no published controlled analysis of the net effect of temperature on biomass-burning OA aging.

3.3. Line and Chamber Wall Losses. Partitioning of vapors to walls in laboratory experiments may alter apparent SOA production: Laboratory results are dependent on losses of both vapors and particles to the chamber walls and instrument/chamber tubing, which influences mass. Each smog chamber analysis in this review has corrected for PWL assuming either that the particles lost to the walls remain in equilibrium with semivolatile vapors ($\omega = 1$) or that vapors only interact with suspended particles ($\omega = 0$): assuming $\omega = 0$ decreases the mean mass enhancement by 3−26% (Figure 1C). In reality, vapor uptake by deposited particles likely lies between the $\omega = 1$ and $\omega = 0$ cases[117] and this remains an uncertainty moving forward. None of the published laboratory studies here correct for partitioning of vapors to walls directly into the Teflon surfaces, which may be more than an order-of-magnitude larger than losses to particles on the walls.[118] The published OFR study does not correct for either particle or vapor wall losses, although these losses are predicted to be relatively low in OFRs.[154−156] We do not correct for vapor wall

DOI: 10.1021/acs.est.9b02588
Environ. Sci. Technol. 2019, 53, 10007−10022

losses in this review as it requires simulating all prior experiments in an aerosol microphysics model and knowledge of chamber turbulence within each experiment. Rather, we rely on the work of Bian et al.[119] in SI Figure S7 to demonstrate the potential importance of correcting for these vapor wall losses (see below).

To date, two published modeling studies have characterized partitioning of vapors to Teflon walls for chamber BB aging experiments.[119,157] Bian et al.[119] modeled both PWL and vapor wall partitioning for the smog chamber in the FLAME III campaign, using size-dependent PWL rates and volatility-dependent vapor partitioning rates.[118] Although uncertainties remained for PWL and vapor partitioning rates, Bian et al.[119] found that simulations without vapor partitioning led to roughly a doubling of OA_{ER} values. SI Figure S7 shows the results from Bian et al.[119] next to the Hennigan et al.[113] results with the vapor-wall-loss corrections lifting the mean and median OA_{ER} values to over 3. In a similar modeling study for the dark period within the chamber before lights are turned on (~75 min), Bian et al.[158] found that over one-third of the initial particle-phase mass was lost during this time to PWL and vapor partitioning, with 35% of this loss coming from evaporation of particles driven by vapor wall losses to the Teflon chamber walls. As vapor partitioning is a function of volatility, these losses could also impact composition markers.

The tubing that transports the smoke between the burn chamber and the smog chambers is also susceptible to losses/delays of gas-phase SOA-precursor material.[159−161] To illustrate this point, we provide a new analysis using the absorptive partitioning model for tubing built by Pagonis et al.[159] ("tubing model") to estimate potential losses of gas-phase material from tubing delay for the smog chamber setup in FLAME III.[113] We assume the fresh-smoke VBS distribution of Bian et al.[119] and the SI provides further details on our methods. At a tubing temperature of 40 °C and residence time of ~4.3 s,[113] the heated aerosol may not achieve equilibrium instantaneously,[162] and we assume two bounding cases on evaporation in which (1) the particles do not evaporate or (2) the particles reach equilibrium instantaneously. For these bounding cases and an initial mass loading of 50 $\mu g\ m^{-3}$, ~16−25% of the S/IVOC gas-phase material does not exit the tubing after 15 min of continual flow of smoke through the tubing (SI Figure S8). This loss increases to ~30% if the tube is not heated. Estimated OA_{ER} values (neglecting further chamber wall losses and making simple assumptions for SOA yields SI) the OA_{ER} ranges between 1.3 and 1.8 for the cases with transfer lines but increase to 2.5 for a case with no assumed tubing loses (SI Figure S8D).

Partitioning of vapors to the chamber walls and tubing decreases the concentrations of gas-phase precursors that could participate in SOA formation, biasing OA_{ER} in laboratory campaigns low (SI Figure S7), further increasing the discrepancies between field and laboratory studies.

3.4. Differences in the Time of the Initial Measurement. Premeasurement chemistry may impact SOA: All of the field and laboratory measurements in Figure 1 are expressed as ratios referenced to an observation that is treated as the initial condition ("time zero"). For field studies, the time after emission at which these initial observations are made can be highly variable between studies, and in some cases significant evaporation and/or chemistry may have occurred prior to that first observation. Generally, the earliest measurements for aircraft campaigns are on the order of ~2−3 min after emission with most being 10 min or more after emission (SI Table S1). In the FIREX laboratory experiments conducted, Koss et al.[13] found a substantial fraction of higher molecular weight organic emissions, including heterocyclic (e.g., furans) and phenolic (e.g., phenol, guaiacol) compounds, that could already have contributed to SOA on these very short time scales.[122] Results for modeling of residential wood combustion indicate the importance of these species to SOA formation,[122] though these results have yet to be tested for ambient BB plumes. As these compounds have short atmospheric lifetimes with respect to OH (~15−60 min), it is possible that some SOA is rapidly formed in the plume after emission but before the "initial" condition of the smoke plume can be measured by aircraft. Furthermore, many plumes undergo relatively rapid dilution during the first several minutes (e.g., vertical mixing into an unstable layer), which may lead to evaporation during this initial time period. Hence, we hypothesize that observed enhancement ratios in the field may be sensitive to the location/timing of the near-field measurement.

Laboratory campaigns have high temporal resolution and can capture early stage chemistry. The time zero in most of the laboratory experiments discussed here occurs when chemistry is initiated (lights are turned on or ozone is added). If rapid reactions are important to BB SOA formation, the differences between time zero in laboratory and field campaigns could be responsible for higher OA_{ER} values in laboratory experiments.

To illustrate how OA_{ER} is sensitive to the definition of time zero, we provide a novel analysis with the FIREX smog chamber data of the impact on OA_{ER} as a function of where time zero is defined relative to when the lights were turned on (Figure 4). Plotted are offsets of 0 (what is always used in laboratory analysis), 10, 30, and 60 min, with the nonzero offsets representative of time zero in field experiments. The OA_{ER} values estimated for a time zero offset of 30 min are about half of these values when there is no offset. For the cases when time zero offset is 60 min after the lights turned on, about a quarter of the experiments have an OA_{ER} less than 1 (only 10 of all reported laboratory OA_{ER} values are less than 1

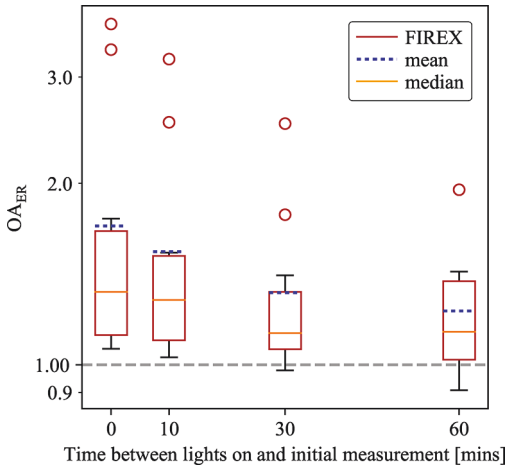

Figure 4. OA enhancement ratios (OA_{ER}) for the FIREX data (ω = 1 case), as a function of where time zero (the initial measurement) is defined (relative to when the lights were turned on, or 0 min). Plotted are offsets of 0 (what is always used in laboratory analysis), 10, 30, and 60 min, with the nonzero offsets representative of time zero in field experiments (SI Table S1). The horizontal dashed gray line at OA_{ER} = 1 indicates no net change in OA mass from the initial mass.

DOI: 10.1021/acs.est.9b02588
Environ. Sci. Technol. 2019, 53, 10007−10022

when there is no offset in time zero). Hence, the FIREX data demonstrate that the difference in definition of time zero in the laboratory experiments and field experiments might explain, at least in part, why OA_{ER} values are generally higher in laboratory experiments than in field experiments. However, the trend shown in Figure 4 could also be due to wall losses of gases, which occur on time scales of 10s of minutes,[118] and thus may not be applicable to field studies. In addition, the BB OFR study of Ortega et al.,[114] found that most of the OA_{ER} increases did not occur on these subhour photochemical time scales. Oxidant concentrations decreased with time during the FIREX smog chamber experiments, which could also favor early OA_{ER} production, but OH has also been observed to decrease in ambient BB plumes with time.[7] As well, initially thick plumes may have low oxidant concentrations due to slow photolysis rates until the plume disperses. More research is needed to understand the initial chemistry occurring in smoke plumes.

4. FUTURE RESEARCH NEEDS

In this study, we have reviewed prior studies of smoke particle aging in the field and lab and discussed hypotheses for differences within and between the two types of studies. In order to create a unified framework to explain variability in the BB aging, we present the following recommendations for key research priorities for the community. We do not rank these priorities, as we hope that ongoing research efforts will guide the relative importance of each priority. We order each subsection by scale, from the molecular level to larger spatial scales:

Under-Characterized Variables in Field Campaigns.

- Better characterization of in-plume chemistry that will allow for improved estimates of, among others, oxidant and radical concentrations, optical thickness, vertical structure, photolysis rates, and reaction rate constants with OH, O_3, and NO_3 for different classes of smoke compounds.
- Consideration of how well variability in source emissions is characterized to obtain an estimate of how much variability would be expected downwind, independent of chemistry.
- Better characterization of the fire size/dilution rate, absolute OA concentrations, and the background aerosol/OA concentration to improve understanding of the influence of these properties on OA aging. A wider range of fire sizes should be sampled from, as field studies thus far appear to have disproportionately sampled midsized fires (Figure 3), and aging may depend on fire size and background concentrations.
- A broader set of study locations, as a majority of existing field studies have occurred in the Americas and a few occurring in Africa. Many important fire-prone biomes remain under-studied including peatlands and moorlands.[128,129]

Under-Characterized Variables in Laboratory Campaigns.

- Better characterization of particle and vapor wall losses for all transfer line and reaction vessel surfaces, and clear documentation of those corrections. Consistent methods for correcting data for each of these losses must also be used to compare across studies.
- A more systematic testing of dilution levels as well as variable temperatures (including rapid changes in temperature) for the same fire conditions in order to understand changes in evaporation and SOA production during plume dilution and temperature changes.
- A wider range of MCEs, as the burn conditions within the available laboratory studies have almost all been with high MCEs, indicating a dominance of flaming fires. More smoldering fires within the laboratory setting should be studied. As well, methods to more closely match field burns should be developed, such as burning more compact fuels/larger amounts, varying fuel water-content, and/or adding heat lamps to increase fuel temperature prior to combustion.
- A wider sampling of fuels as laboratory studies have been focused predominantly on fuels that may exist in North American fires.

Reconciling Laboratory and Field Campaigns.

- Expanding use of emerging techniques that allow molecular-level measurements of OA in real-time[163] should be applied to both field and lab studies to allow more direct connections than can be made with using only OA and O:C to characterize the composition of emissions.
- Increased reporting and analysis of emissions correlations such as the high- and low-temperature emissions profiles of VOCs identified by Sekimoto et al.[127] These profiles provide tractable methods that can be compared in field and laboratory campaigns for understanding the thousands of compounds emitted in fires and could be applied to aging studies in order to determine which correlations may increase understanding of aged smoke.
- Better characterization of the OA evolution of individual fuels for variable starting mass concentrations to explore more dilution regimes in laboratory experiments. As observed for the FLAME III OFR data, more SOA was formed with a lower initial POA concentration (increased dilution), likely due to more available precursors.[12,114] Careful observation of both mass and compositional changes in these experiments can test the impacts of dilution on smoke aging.
- Expanded use of OFRs, given their relative ease-of-use compared to environmental chambers. In lab studies, OFRs can provide anticipated particle mass, composition markers, and size distribution changes with variable levels of aging[164] for the same fuel or fuels burned. In field studies, OFRs can be set up at ground-based sites to sample directly from ground-level plumes and have also successfully operated from aircraft.[99] Aging information from field OFRs could be directly compared to aircraft observations of the downwind plume.
- Models as tools to interpret field measurements. Models can help to understand the chemical and physical impacts of dilution in plumes. As well, combinations of modeling and laboratory efforts can constrain initial, fast chemistry anticipated in smoke plumes and should be then applied to field measurements in order to determine anticipated changes in mass and composition that can occur between the time of emission and the time of the initial field measurements

DOI: 10.1021/acs.est.9b02588
Environ. Sci. Technol. 2019, 53, 10007−10022

■ ASSOCIATED CONTENT

Supporting Information

The Supporting Information is available free of charge on the ACS Publications website at DOI: 10.1021/acs.est.9b02588.

Additional information as noted in the text (PDF)

■ AUTHOR INFORMATION

Corresponding Author

*E-mail: Anna.Hodshire@colostate.edu.

ORCID

Anna L. Hodshire: 0000-0002-5099-3659
Shantanu H. Jathar: 0000-0003-4106-2358
Jose L. Jimenez: 0000-0001-6203-1847
Timothy B. Onasch: 0000-0001-7796-7840
Jeffrey R. Pierce: 0000-0002-4241-838X

Present Address

▽(A.M.O.) Air Pollution Control Division, Colorado Department of Public Health and Environment, Denver, Colorado 80246, United States.

Author Contributions

The manuscript was written through contributions of all authors. All authors have given approval to the final version of the manuscript.

Notes

The authors declare no competing financial interest.

■ ACKNOWLEDGMENTS

A.L.H., J.R.P., S.M.K., A.A., S.J.H., M.J.A., B.B.S., and C.R.L. received support from the U.S NOAA, an Office of Science, Office of Atmospheric Chemistry, Carbon Cycle, and Climate Program, under the cooperative agreement award nos. NA17OAR430001, NA17OAR4310002, and NA17OAR4310003; the U.S. NSF Atmospheric Chemistry program, under grant nos. AGS-1559607, AGS-1558966, AGS-1830748, and AGS-1559598; the Joint Fire Science Program under project 14-1-03-26; and Office of Naval Research under #N00014-16-1-2040. T.B.O. acknowledges NOAA contract no. NA16OAR4310104 (to Aerodyne) J.L.J. acknowledges NASA 80NSSC18K0630, and NSF AGS-1822664. Additionally, J.L.J. and A.M.O. acknowledge the DOE (BER, ASP Program DE-SC0006035) and the EPA (STAR grant R833747) for funding for FLAME-III and A.M.O.'s graduate fellowship from the DOE SCGP Fellowship Program (ORAU, ORISE). The EPA has not reviewed this manuscript and no endorsement should be inferred. We thank Liam Lewane, Abril Galang, and Shiva Tarun for help with the environmental chamber experiments during FIREX-2016, and Scott Herndon and the Aerodyne Mobile Laboratory crew. We also thank Adam Ahern for providing additional FLAME-IV analyses.

■ REFERENCES

(1) Scott, A. C.; Glasspool, I. J. The Diversification of Paleozoic Fire Systems and Fluctuations in Atmospheric Oxygen Concentration. *Proc. Natl. Acad. Sci. U. S. A.* **2006**, *103* (29), 10861−10865.

(2) Randerson, J. T.; Chen, Y.; van der Werf, G. R.; Rogers, B. M.; Morton, D. C. Global burned area and biomass burning emissions from small fires: Burned area from small fires. *J. Geophys. Res.* **2012**, *117* (G4). n/a.

(3) Baker, K. R.; Woody, M. C.; Tonnesen, G. S.; Hutzell, W.; Pye, H. O. T.; Beaver, M. R.; Pouliot, G.; Pierce, T. Contribution of Regional-Scale Fire Events to Ozone and PM2.5 Air Quality Estimated by Photochemical Modeling Approaches. *Atmos. Environ.* **2016**, *140*, 539−554.

(4) Gilman, J. B.; Lerner, B. M.; Kuster, W. C.; Goldan, P. D.; Warneke, C.; Veres, P. R.; Roberts, J. M.; Gouw, J. A.; Burling, I. R.; Yokelson, R. J. Biomass Burning Emissions and Potential Air Quality Impacts of Volatile Organic Compounds and Other Trace Gases from Fuels Common in the US. *Atmos. Chem. Phys.* **2015**, *15* (24), 13915−13938.

(5) Akagi, S. K.; Yokelson, R. J.; Wiedinmyer, C.; Alvarado, M. J.; Reid, J. S.; Karl, T.; Crounse, J. D.; Wennberg, P. O. Emission Factors for Open and Domestic Biomass Burning for Use in Atmospheric Models. *Atmos. Chem. Phys.* **2011**, *11* (9), 4039−4072.

(6) Reid, J. S.; Koppmann, R.; Eck, T. F.; Eleuterio, D. P. A Review of Biomass Burning Emissions Part II: Intensive Physical Properties of Biomass Burning Particles. *Atmos. Chem. Phys.* **2005**, *5* (3), 799−825.

(7) Yokelson, R. J.; Crounse, J. D.; DeCarlo, P. F.; Karl, T.; Urbanski, S.; Atlas, E.; Campos, T.; Shinozuka, Y.; Kapustin, V.; Clarke, A. D.; et al. Emissions from Biomass Burning in the Yucatan. *Atmos. Chem. Phys.* **2009**, *9* (15), 5785−5812.

(8) Yokelson, R. J.; Burling, I. R.; Urbanski, S. P.; Atlas, E. L.; Adachi, K.; Buseck, P. R.; Wiedinmyer, C.; Akagi, S. K.; Toohey, D. W.; Wold, C. E. Trace Gas and Particle Emissions from Open Biomass Burning in Mexico. *Atmos. Chem. Phys.* **2011**, *11* (14), 6787−6808.

(9) Jen, C. N.; Hatch, L. E.; Selimovic, V.; Yokelson, R. J.; Weber, R.; Fernandez, A. E.; Kreisberg, N. M.; Barsanti, K. C.; Goldstein, A. H. Speciated and Total Emission Factors of Particulate Organics from Burning Western US Wildland Fuels and Their Dependence on Combustion Efficiency. *Atmos. Chem. Phys.* **2019**, *19* (2), 1013−1026.

(10) Hatch, L. E.; Luo, W.; Pankow, J. F.; Yokelson, R. J.; Stockwell, C. E.; Barsanti, K. C. Identification and Quantification of Gaseous Organic Compounds Emitted from Biomass Burning Using Two-Dimensional Gas Chromatography–Time-of-Flight Mass Spectrometry. *Atmos. Chem. Phys.* **2015**, *15* (4), 1865−1899.

(11) Hatch, L. E.; Yokelson, R. J.; Stockwell, C. E.; Veres, P. R.; Simpson, I. J.; Blake, D. R.; Orlando, J. J.; Barsanti, K. C. Multi-Instrument Comparison and Compilation of Non-Methane Organic Gas Emissions from Biomass Burning and Implications for Smoke-Derived Secondary Organic Aerosol Precursors. *Atmos. Chem. Phys.* **2017**, *17* (2), 1471−1489.

(12) Hatch, L. E.; Rivas-Ubach, A.; Jen, C. N.; Lipton, M.; Goldstein, A. H.; Barsanti, K. C. Measurements of I/SVOCs in Biomass-Burning Smoke Using Solid-Phase Extraction Disks and Two-Dimensional Gas Chromatography. *Atmos. Chem. Phys.* **2018**, *18* (24), 17801−17817.

(13) Koss, A. R.; Sekimoto, K.; Gilman, J. B.; Selimovic, V.; Coggon, M. M.; Zarzana, K. J.; Yuan, B.; Lerner, B. M.; Brown, S. S.; Jimenez, J. L.; et al. Non-Methane Organic Gas Emissions from Biomass Burning: Identification, Quantification, and Emission Factors from PTR-ToF during the FIREX 2016 Laboratory Experiment. *Atmos. Chem. Phys.* **2018**, *18* (5), 3299−3319.

(14) Dreessen, J.; Sullivan, J.; Delgado, R. Observations and Impacts of Transported Canadian Wildfire Smoke on Ozone and Aerosol Air Quality in the Maryland Region on June 9−12, 2015. *J. Air Waste Manage. Assoc.* **2016**, *66* (9), 842−862.

(15) Bytnerowicz, A.; Hsu, Y.-M.; Percy, K.; Legge, A.; Fenn, M. E.; Schilling, S.; Frączek, W.; Alexander, D. Ground-Level Air Pollution Changes during a Boreal Wildland Mega-Fire. *Sci. Total Environ.* **2016**, *572*, 755−769.

(16) Lewis, K. A.; Arnott, W. P.; Moosmüller, H.; Chakrabarty, R. K.; Carrico, C. M.; Kreidenweis, S. M.; Day, D. E.; Malm, W. C.; Laskin, A.; Jimenez, J. L.; et al. Reduction in Biomass Burning Aerosol Light Absorption upon Humidification: Roles of Inorganically-Induced Hygroscopicity, Particle Collapse, and Photoacoustic Heat and Mass Transfer. *Atmos. Chem. Phys.* **2009**, *9* (22), 8949−8966.

(17) Akagi, S. K.; Craven, J. S.; Taylor, J. W.; McMeeking, G. R.; Yokelson, R. J.; Burling, I. R.; Urbanski, S. P.; Wold, C. E.; Seinfeld, J. H.; Coe, H.; et al. Evolution of Trace Gases and Particles Emitted by

DOI: 10.1021/acs.est.9b02588
Environ. Sci. Technol. 2019, 53, 10007−10022

a Chaparral Fire in California. *Atmos. Chem. Phys.* **2012**, *12* (3), 1397−1421.
(18) Alvarado, M. J.; Lonsdale, C. R.; Yokelson, R. J.; Akagi, S. K.; Coe, H.; Craven, J. S.; Fischer, E. V.; McMeeking, G. R.; Seinfeld, J. H.; Soni, T.; et al. Investigating the Links between Ozone and Organic Aerosol Chemistry in a Biomass Burning Plume from a Prescribed Fire in California Chaparral. *Atmos. Chem. Phys.* **2015**, *15* (12), 6667−6688.
(19) Hecobian, A.; Liu, Z.; Hennigan, C. J.; Huey, L. G.; Jimenez, J. L.; Cubison, M. J.; Vay, S.; Diskin, G. S.; Sachse, G. W.; Wisthaler, A.; et al. Comparison of Chemical Characteristics of 495 Biomass Burning Plumes Intercepted by the NASA DC-8 Aircraft during the ARCTAS/CARB-2008 Field Campaign. *Atmos. Chem. Phys.* **2011**, *11* (24), 13325−13337.
(20) Sakamoto, K. M.; Laing, J. R.; Stevens, R. G.; Jaffe, D. A.; Pierce, J. R. The Evolution of Biomass-Burning Aerosol Size Distributions due to Coagulation: Dependence on Fire and Meteorological Details and Parameterization. *Atmos. Chem. Phys.* **2016**, *16* (12), 7709−7724.
(21) Vakkari, V.; Kerminen, V.-M.; Beukes, J. P.; Tiitta, P.; van Zyl, P. G.; Josipovic, M.; Venter, A. D.; Jaars, K.; Worsnop, D. R.; Kulmala, M.; et al. Rapid Changes in Biomass Burning Aerosols by Atmospheric Oxidation. *Geophys. Res. Lett.* **2014**, *41* (7), 2644−2651.
(22) Vakkari, V.; Beukes, J. P.; Dal Maso, M.; Aurela, M.; Josipovic, M.; van Zyl, P. G. Major Secondary Aerosol Formation in Southern African Open Biomass Burning Plumes. *Nat. Geosci.* **2018**, *11* (8), 580−583.
(23) Brito, J.; Rizzo, L. V.; Morgan, W. T.; Coe, H.; Johnson, B.; Haywood, J.; Longo, K.; Freitas, S.; Andreae, M. O.; Artaxo, P. Ground-Based Aerosol Characterization during the South American Biomass Burning Analysis (SAMBBA) Field Experiment. *Atmos. Chem. Phys.* **2014**, *14* (22), 12069−12083.
(24) Capes, G.; Johnson, B.; McFiggans, G.; Williams, P. I.; Haywood, J.; Coe, H. Aging of biomass burning aerosols over West Africa: Aircraft measurements of chemical composition, microphysical properties, and emission ratios. *J. Geophys. Res.* **2008**, *113* (D23). DOI: 10.1029/2008JD009845
(25) Collier, S.; Zhou, S.; Onasch, T. B.; Jaffe, D. A.; Kleinman, L.; Sedlacek, A. J., 3rd; Briggs, N. L.; Hee, J.; Fortner, E.; Shilling, J. E.; et al. Regional Influence of Aerosol Emissions from Wildfires Driven by Combustion Efficiency: Insights from the BBOP Campaign. *Environ. Sci. Technol.* **2016**, *50* (16), 8613−8622.
(26) Cubison, M. J.; Ortega, A. M.; Hayes, P. L.; Farmer, D. K.; Day, D.; Lechner, M. J.; Brune, W. H.; Apel, E.; Diskin, G. S.; Fisher, J. A.; et al. Effects of Aging on Organic Aerosol from Open Biomass Burning Smoke in Aircraft and Laboratory Studies. *Atmos. Chem. Phys.* **2011**, *11* (23), 12049−12064.
(27) Forrister, H.; Liu, J.; Scheuer, E.; Dibb, J.; Ziemba, L.; Thornhill, K. L.; Anderson, B.; Diskin, G.; Perring, A. E.; Schwarz, J. P.; et al. Evolution of Brown Carbon in Wildfire Plumes. *Geophys. Res. Lett.* **2015**, *42* (11), 4623−4630.
(28) Liu, X.; Zhang, Y.; Huey, L. G.; Yokelson, R. J.; Wang, Y.; Jimenez, J. L.; Campuzano-Jost, P.; Beyersdorf, A. J.; Blake, D. R.; Choi, Y.; et al. Agricultural Fires in the Southeastern US during SEAC4RS: Emissions of Trace Gases and Particles and Evolution of Ozone, Reactive Nitrogen, and Organic Aerosol. *J. Geophys. Res. D: Atmos.* **2016**, *121* (12), 7383−7414.
(29) May, A. A.; Lee, T.; McMeeking, G. R.; Akagi, S.; Sullivan, A. P.; Urbanski, S.; Yokelson, R. J.; Kreidenweis, S. M. Observations and Analysis of Organic Aerosol Evolution in Some Prescribed Fire Smoke Plumes. *Atmos. Chem. Phys.* **2015**, *15* (11), 6323−6335.
(30) Sakamoto, K. M.; Allan, J. D.; Coe, H.; Taylor, J. W.; Duck, T. J.; Pierce, J. R. Aged Boreal Biomass-Burning Aerosol Size Distributions from BORTAS 2011. *Atmos. Chem. Phys.* **2015**, *15* (4), 1633−1646.
(31) Zhou, S.; Collier, S.; Jaffe, D. A.; Briggs, N. L.; Hee, J.; Sedlacek, A. J., III; Kleinman, L.; Onasch, T. B.; Zhang, Q. Regional Influence of Wildfires on Aerosol Chemistry in the Western US and Insights into Atmospheric Aging of Biomass Burning Organic Aerosol. *Atmos. Chem. Phys.* **2017**, *17* (3), 2477−2493.
(32) Hobbs, P. V.; Sinha, P.; Yokelson, R. J.; Christian, T. J.; Blake, D. R.; Gao, S.; Kirchstetter, T. W.; Novakov, T.; Pilewskie, P. Evolution of gases and particles from a savanna fire in South Africa. *J. Geophys. Res. D, Atmos.* **2003**, *108* (D13).n/a
(33) Jolleys, M. D.; Coe, H.; McFiggans, G.; Capes, G.; Allan, J. D.; Crosier, J.; Williams, P. I.; Allen, G.; Bower, K. N.; Jimenez, J. L.; et al. Characterizing the Aging of Biomass Burning Organic Aerosol by Use of Mixing Ratios: A Meta-Analysis of Four Regions. *Environ. Sci. Technol.* **2012**, *46* (24), 13093−13102.
(34) Jolleys, M. D.; Coe, H.; McFiggans, G.; Taylor, J. W.; O'Shea, S. J.; Le Breton, M.; Bauguitte, S. J.-B.; M?ller, S.; Di Carlo, P.; Aruffo, E.; et al. Properties and Evolution of Biomass Burning Organic Aerosol from Canadian Boreal Forest Fires. *Atmos. Chem. Phys.* **2015**, *15* (6), 3077−3095.
(35) Cachier, H.; Liousse, C.; Buat-Menard, P.; Gaudichet, A. Particulate Content of Savanna Fire Emissions. *J. Atmos. Chem.* **1995**, *22* (1−2), 123−148.
(36) Formenti, P.; Elbert, W.; Maenhaut, W.; Haywood, J.; Osborne, S.; Andreae, M. O. Inorganic and carbonaceous aerosols during the Southern African Regional Science Initiative (SAFARI 2000) experiment: Chemical characteristics, physical properties, and emission data for smoke from African biomass burning. *J. Geophys. Res. D: Atmos.* **2003**, *108* (D13).n/a
(37) Nance, J. D.; Hobbs, P. V.; Radke, L. F.; Ward, D. E. Airborne Measurements of Gases and Particles from an Alaskan Wildfire. *J. Geophys. Res.* **1993**, *98* (D8), 14873.
(38) Reid, J. S.; Hobbs, P. V.; Ferek, R. J.; Blake, D. R.; Martins, J. V.; Dunlap, M. R.; Liousse, C. Physical, Chemical, and Optical Properties of Regional Hazes Dominated by Smoke in Brazil. *J. Geophys. Res.* **1998**, *103* (D24), 32059−32080.
(39) Martin, M. V.; Honrath, R. E.; Owen, R. C.; Pfister, G.; Fialho, P.; Barata, F. Significant enhancements of nitrogen oxides, black carbon, and ozone in the North Atlantic lower free troposphere resulting from North American boreal wildfires. *J. Geophys. Res. D, Atmos.* **2006**, *111* (D23).n/a
(40) Voulgarakis, A.; Field, R. D. Fire Influences on Atmospheric Composition, Air Quality and Climate. *Current Pollution Reports* **2015**, *1* (2), 70−81.
(41) Mallia, D. V.; Lin, J. C.; Urbanski, S.; Ehleringer, J.; Nehrkorn, T. Impacts of Upwind Wildfire Emissions on CO, CO2, and PM2. 5 Concentrations in Salt Lake City, Utah. *J. Geophys. Res. D: Atmos.* **2015**, *120* (1), 147−166.
(42) Lindaas, J.; Farmer, D. K.; Pollack, I. B.; Abeleira, A.; Flocke, F.; Roscioli, R.; Herndon, S.; Fischer, E. V. Changes in Ozone and Precursors during Two Aged Wildfire Smoke Events in the Colorado Front Range in Summer 2015. *Atmos. Chem. Phys.* **2017**, *17* (17), 10691−10707.
(43) Lei, W.; Li, G.; Molina, L. T. Modeling the Impacts of Biomass Burning on Air Quality in and around Mexico City. *Atmos. Chem. Phys.* **2013**, *13* (5), 2299−2319.
(44) Landis, M. S.; Edgerton, E. S.; White, E. M.; Wentworth, G. R.; Sullivan, A. P.; Dillner, A. M. The Impact of the 2016 Fort McMurray Horse River Wildfire on Ambient Air Pollution Levels in the Athabasca Oil Sands Region, Alberta, Canada. *Sci. Total Environ.* **2018**, *618*, 1665−1676.
(45) Garofalo, L. A.; Pothier, M. A.; Levin, E. J. T.; Campos, T.; Kreidenweis, S. M.; Farmer, D. K. Emission and Evolution of Submicron Organic Aerosol in Smoke from Wildfires in the Western United States. *ACS Earth Space Chem.* **2019**, *3*, 1237.
(46) Briggs, N. L.; Jaffe, D. A.; Gao, H.; Hee, J. R.; Baylon, P. M.; Zhang, Q.; Zhou, S.; Collier, S. C.; Sampson, P. D.; Cary, R. A. Particulate matter, ozone, and nitrogen species in aged wildfire plumes observed at the mount bachelor observatory. *Aerosol Air Qual. Res.* **2016**, *16* (12).3075
(47) Decker, Z. C. J.; Zarzana, K. J.; Coggon, M.; Min, K.-E.; Pollack, I.; Ryerson, T. B.; Peischl, J.; Edwards, P.; Dubé, W. P.; Markovic, M. Z.; et al. Nighttime Chemical Transformation in

Biomass Burning Plumes: A Box Model Analysis Initialized with Aircraft Observations. *Environ. Sci. Technol.* **2019**, *53* (5), 2529−2538.
(48) Bond, T. C.; Doherty, S. J.; Fahey, D. W.; Forster, P. M.; Berntsen, T.; DeAngelo, B. J.; Flanner, M. G.; Ghan, S.; Kärcher, B.; Koch, D.; et al. Bounding the Role of Black Carbon in the Climate System: A Scientific. *Assessment. J. Geophys. Res. D: Atmos.* **2013**, *118* (11), 5380−5552.
(49) Voulgarakis, A.; Marlier, M. E.; Faluvegi, G.; Shindell, D. T.; Tsigaridis, K.; Mangeon, S. Interannual Variability of Tropospheric Trace Gases and Aerosols: The Role of Biomass Burning Emissions. *J. Geophys. Res. D: Atmos.* **2015**, *120* (14), 7157−7173.
(50) Ramnarine, E.; Kodros, J. K.; Hodshire, A. L.; Lonsdale, C. R.; Alvarado, M. J.; Pierce, J. R. Effects of near-Source Coagulation of Biomass Burning Aerosols on Global Predictions of Aerosol Size Distributions and Implications for Aerosol Radiative Effects. *Atmos. Chem. Phys.* **2019**, *19* (9), 6561−6577.
(51) Jaffe, D. A.; Wigder, N. L. Ozone Production from Wildfires: A Critical Review. *Atmos. Environ.* **2012**, *51*, 1−10.
(52) Nie, W.; Ding, A. J.; Xie, Y. N.; Xu, Z.; Mao, H.; Kerminen, V.-M.; Zheng, L. F.; Qi, X. M.; Huang, X.; Yang, X.-Q.; et al. Influence of Biomass Burning Plumes on HONO Chemistry in Eastern China. *Atmos. Chem. Phys.* **2015**, *15* (3), 1147−1159.
(53) Xie, Y.; Ding, A.; Nie, W.; Mao, H.; Qi, X.; Huang, X.; Xu, Z.; Kerminen, V.-M.; Petäjä, T.; Chi, X.; et al. Enhanced Sulfate Formation by Nitrogen Dioxide: Implications from in Situ Observations at the SORPES Station. *J. Geophys. Res. D: Atmos.* **2015**, *120* (24), 12679−12694.
(54) Brey, S. J.; Barnes, E. A.; Pierce, J. R.; Wiedinmyer, C.; Fischer, E. V. Environmental Conditions, Ignition Type, and Air Quality Impacts of Wildfires in the Southeastern and Western United States. *Earth's Future* **2018**, *6* (10), 1442−1456.
(55) Lassman, W.; Ford, B.; Gan, R. W.; Pfister, G.; Magzamen, S.; Fischer, E. V.; Pierce, J. R. Spatial and Temporal Estimates of Population Exposure to Wildfire Smoke during the Washington State 2012 Wildfire Season Using Blended Model, Satellite, and in Situ Data: Multimethod Estimates of Smoke Exposure. *GeoHealth* **2017**, *1* (3), 106−121.
(56) Janssen, N. A. H.Joint, W. H. O. *Health Effects of Black Carbon*; WHO Regional Office for Europe Copenhagen, 2012.
(57) Johnston, F. H.; Henderson, S. B.; Chen, Y.; Randerson, J. T.; Marlier, M.; Defries, R. S.; Kinney, P.; Bowman, D. M. J. S.; Brauer, M. Estimated Global Mortality Attributable to Smoke from Landscape Fires. *Environ. Health Perspect.* **2012**, *120* (5), 695−701.
(58) Naeher, L. P.; Brauer, M.; Lipsett, M.; Zelikoff, J. T. Woodsmoke Health Effects: A Review. *Inhalation Toxicol.* **2007**, *19*, 67.
(59) Zhang, Y.; Tao, S.; Shen, H.; Ma, J. Inhalation Exposure to Ambient Polycyclic Aromatic Hydrocarbons and Lung Cancer Risk of Chinese Population. *Proc. Natl. Acad. Sci. U. S. A.* **2009**, *106* (50), 21063−21067.
(60) Roberts, J. M.; Veres, P. R.; Cochran, A. K. Isocyanic acid in the atmosphere and its possible link to smoke-related health effects. *Proc. Natl. Acad. Sci.* **2011**.*1082289668971*
(61) Samburova, V.; Connolly, J.; Gyawali, M.; Yatavelli, R. L. N.; Watts, A. C.; Chakrabarty, R. K.; Zielinska, B.; Moosmüller, H.; Khlystov, A. Polycyclic Aromatic Hydrocarbons in Biomass-Burning Emissions and Their Contribution to Light Absorption and Aerosol Toxicity. *Sci. Total Environ.* **2016**, *568*, 391−401.
(62) Ford, B.; Val Martin, M.; Zelasky, S. E.; Fischer, E. V.; Anenberg, S. C.; Heald, C. L.; Pierce, J. R. Future Fire Impacts on Smoke Concentrations, Visibility, and Health in the Contiguous United States. *GeoHealth* **2018**, *2* (8), 229−247.
(63) Charlson, R. J.; Schwartz, S. E.; Hales, J. M.; Cess, R. D.; Coakley, J. A., Jr; Hansen, J. E.; Hofmann, D. J. Climate Forcing by Anthropogenic Aerosols. *Science* **1992**, *255* (5043), 423−430.
(64) Heald, C. L.; Ridley, D. A.; Kroll, J. H.; Barrett, S. R. H.; Cady-Pereira, K. E.; Alvarado, M. J.; Holmes, C. D. Contrasting the Direct Radiative Effect and Direct Radiative Forcing of Aerosols. *Atmos. Chem. Phys.* **2014**, *14* (11), 5513−5527.
(65) Twomey, S. Pollution and the Planetary Albedo. *Atmos. Environ.* **2007**, *41*, 120−125.
(66) Boucher, O.; Randall, D.; Artaxo, P.; Bretherton, C.; Feingold, G.; Forster, P.; Kerminen, V.-M.; Kondo, Y.; Liao, H.; Lohmann, U.; et al. Clouds and Aerosols. In *Climate change 2013: The Physical Science Basis. Contribution of Working Group I to the Fifth Assessment Report of the Intergovernmental Panel on Climate Change*; Cambridge University Press, 2013; pp 571−657.
(67) Petters, M. D.; Carrico, C. M.; Kreidenweis, S. M.; Prenni, A. J.; DeMott, P. J.; Collett, J. L., Jr; Moosmüller, H. Cloud condensation nucleation activity of biomass burning aerosol. *J. Geophys. Res.* **2009**, *114* (D22). DOI: 10.1029/2009JD012353
(68) DeMott, P. J.; Petters, M. D.; Prenni, A. J.; Carrico, C. M.; Kreidenweis, S. M.; Collett, J. L., Jr.; Moosmüller, H. Ice Nucleation Behavior of Biomass Combustion Particles at Cirrus Temperatures. *J. Geophys. Res.* **2009**, *114* (D16), 1770.
(69) Petters, M. D.; Kreidenweis, S. M. A Single Parameter Representation of Hygroscopic Growth and Cloud Condensation Nucleus Activity. *Atmos. Chem. Phys.* **2007**, *7* (8), 1961−1971.
(70) Seinfeld, J. H.; Pandis, S. N. *Atmospheric Chemistry and Physics: From Air Pollution to Climate Change*; John Wiley & Sons, 2016.
(71) Kasischke, E. S.; Turetsky, M. R. Recent Changes in the Fire Regime across the North American Boreal region—Spatial and Temporal Patterns of Burning across Canada and Alaska. *Geophys. Res. Lett.* **2006**, *33* (9), 1996.
(72) Westerling, A. L. Increasing western US Forest wildfire activity: sensitivity to changes in the timing of spring. *Philos. Trans. R. Soc., B* **2016**, *371* (1696). 20150178.
(73) Liu, J. C.; Mickley, L. J.; Sulprizio, M. P.; Dominici, F.; Yue, X.; Ebisu, K.; Anderson, G. B.; Khan, R. F. A.; Bravo, M. A.; Bell, M. L. Particulate Air Pollution from Wildfires in the Western US under Climate Change. *Clim. Change* **2016**, *138* (3), 655−666.
(74) Yue, X.; Mickley, L. J.; Logan, J. A.; Kaplan, J. O. Ensemble Projections of Wildfire Activity and Carbonaceous Aerosol Concentrations over the Western United States in the Mid-21st Century. *Atmos. Environ.* **2013**, *77*, 767−780.
(75) McClure, C. D.; Jaffe, D. A. US Particulate Matter Air Quality Improves except in Wildfire-Prone Areas. *Proc. Natl. Acad. Sci. U. S. A.* **2018**, *115* (31), 7901−7906.
(76) O'Dell, K.; Ford, B.; Fischer, E. V.; Pierce, J. R. Contribution of Wildland-Fire Smoke to US PM2.5 and Its Influence on Recent Trends. *Environ. Sci. Technol.* **2019**, *53* (4), 1797−1804.
(77) Morgan, W. T.; Allan, J. D.; Bauguitte, S.; Darbyshire, E.; Flynn, M. J.; Lee, J.; Liu, D.; Johnson, B.; Haywood, J.; Longo, K. M.; et al. Transformation and Aging of Biomass Burning Carbonaceous Aerosol over Tropical South America from Aircraft in-Situ Measurements during SAMBBA. *Atmos. Chem. Phys. Discuss.* **2019**, 1−32.
(78) Goldstein, A. H.; Galbally, I. E. Known and Unexplored Organic Constituents in the Earth's Atmosphere. *Environ. Sci. Technol.* **2007**, *41* (5), 1514−1521.
(79) Shiraiwa, M.; Berkemeier, T.; Schilling-Fahnestock, K. A.; Seinfeld, J. H.; Pöschl, U. Molecular Corridors and Kinetic Regimes in the Multiphase Chemical Evolution of Secondary Organic Aerosol. *Atmos. Chem. Phys.* **2014**, *14* (16), 8323−8341.
(80) Pankow, J. F. An Absorption Model of Gas/particle Partitioning of Organic Compounds in the Atmosphere. *Atmos. Environ.* **1994**, *28* (2), 185−188.
(81) Odum, J. R.; Hoffmann, T.; Bowman, F.; Collins, D.; Flagan, R. C.; Seinfeld, J. H. Gas/Particle Partitioning and Secondary Organic Aerosol Yields. *Environ. Sci. Technol.* **1996**, *30* (8), 2580−2585.
(82) Donahue, N. M.; Robinson, A. L.; Stanier, C. O.; Pandis, S. N. Coupled Partitioning, Dilution, and Chemical Aging of Semivolatile Organics. *Environ. Sci. Technol.* **2006**, *40* (8), 2635−2643.
(83) Murphy, B. N.; Donahue, N. M.; Robinson, A. L.; Pandis, S. N. A Naming Convention for Atmospheric Organic Aerosol. *Atmos. Chem. Phys.* **2014**, *14* (11), 5825−5839.
(84) Kroll, J. H.; Smith, J. D.; Che, D. L.; Kessler, S. H.; Worsnop, D. R.; Wilson, K. R. Measurement of Fragmentation and Functionalization Pathways in the Heterogeneous Oxidation of

DOI: 10.1021/acs.est.9b02588
Environ. Sci. Technol. 2019, 53, 10007−10022

Oxidized Organic Aerosol. *Phys. Chem. Chem. Phys.* **2009**, *11* (36), 8005−8014.
(85) Donahue, N. M.; Trump, E. R.; Pierce, J. R.; Riipinen, I. Theoretical constraints on pure vapor-pressure driven condensation of organics to ultrafine particles. *Geophys. Res. Lett.* **2011**, *38* (16).n/a
(86) Jathar, S. H.; Cappa, C. D.; Wexler, A. S.; Seinfeld, J. H.; Kleeman, M. J. Multi-Generational Oxidation Model to Simulate Secondary Organic Aerosol in a 3-D Air Quality Model. *Geosci. Model Dev.* **2015**, *8* (8), 2553−2567.
(87) Zhang, X.; Cappa, C. D.; Jathar, S. H.; McVay, R. C.; Ensberg, J. J.; Kleeman, M. J.; Seinfeld, J. H. Influence of Vapor Wall Loss in Laboratory Chambers on Yields of Secondary Organic Aerosol. *Proc. Natl. Acad. Sci. U. S. A.* **2014**, *111* (16), 5802−5807.
(88) Shiraiwa, M.; Seinfeld, J. H. Equilibration timescale of atmospheric secondary organic aerosol partitioning. *Geophys. Res. Lett.* **2012**, *39* (24). DOI: 10.1029/2012GL054008.
(89) Zaveri, R. A.; Easter, R. C.; Shilling, J. E.; Seinfeld, J. H. Modeling Kinetic Partitioning of Secondary Organic Aerosol and Size Distribution Dynamics: Representing Effects of Volatility, Phase State, and Particle-Phase Reaction. *Atmos. Chem. Phys.* **2014**, *14* (10), 5153−5181.
(90) DeCarlo, P. F.; Dunlea, E. J.; Kimmel, J. R.; Aiken, A. C.; Sueper, D.; Crounse, J.; Wennberg, P. O.; Emmons, L.; Shinozuka, Y.; Clarke, A.; et al. Fast Airborne Aerosol Size and Chemistry Measurements above Mexico City and Central Mexico during the MILAGRO Campaign. *Atmos. Chem. Phys.* **2008**, *8* (14), 4027−4048.
(91) Reddington, C. L.; Spracklen, D. V.; Artaxo, P.; Ridley, D. A.; Rizzo, L. V.; Arana, A. Analysis of Particulate Emissions from Tropical Biomass Burning Using a Global Aerosol Model and Long-Term Surface Observations. *Atmos. Chem. Phys.* **2016**, *16* (17), 11083−11106.
(92) Shrivastava, M.; Easter, R. C.; Liu, X.; Zelenyuk, A.; Singh, B.; Zhang, K.; Ma, P.-L.; Chand, D.; Ghan, S.; Jimenez, J. L.; et al. Global Transformation and Fate of SOA: Implications of Low-Volatility SOA and Gas-Phase Fragmentation Reactions. *J. Geophys. Res. D: Atmos.* **2015**, *120* (9), 4169−4195.
(93) Konovalov, I. B.; Beekmann, M.; Berezin, E. V.; Petetin, H.; Mielonen, T.; Kuznetsova, I. N.; Andreae, M. O. The Role of Semi-Volatile Organic Compounds in the Mesoscale Evolution of Biomass Burning Aerosol: A Modeling Case Study of the 2010 Mega-Fire Event in Russia. *Atmos. Chem. Phys.* **2015**, *15* (23), 13269−13297.
(94) Konovalov, I. B.; Beekmann, M.; Berezin, E. V.; Formenti, P.; Andreae, M. O. Probing into the Aging Dynamics of Biomass Burning Aerosol by Using Satellite Measurements of Aerosol Optical Depth and Carbon Monoxide. *Atmos. Chem. Phys.* **2017**, *17* (7), 4513−4537.
(95) Koplitz, S. N.; Nolte, C. G.; Pouliot, G. A.; Vukovich, J. M.; Beidler, J. Influence of Uncertainties in Burned Area Estimates on Modeled Wildland Fire PM2.5 and Ozone Pollution in the Contiguous U.S. *Atmos. Environ.* **2018**, *191*, 328−339.
(96) Griffin, R. J.; Chen, J.; Carmody, K.; Vutukuru, S.; Dabdub, D. Contribution of gas phase oxidation of volatile organic compounds to atmospheric carbon monoxide levels in two areas of the United States. *J. Geophys. Res. D, Atmos.* **2007**, *112* (D10). DOI: 10.1029/2006JD007602
(97) Alvarado, M. J.; Prinn, R. G. Formation of Ozone and Growth of Aerosols in Young Smoke Plumes from Biomass Burning: 1. Lagrangian Parcel Studies. *J. Geophys. Res.* **2009**, *114* (D9), D09307.
(98) Gouw, J.; Jimenez, J. L. Organic Aerosols in the Earth's Atmosphere. *Environ. Sci. Technol.* **2009**, *43* (20), 7614−7618.
(99) Nault, B. A.; Campuzano-Jost, P.; Day, D. A.; Schroder, J. C.; Anderson, B.; Beyersdorf, A. J.; Blake, D. R.; Brune, W. H.; Choi, Y.; Corr, C. A.; et al. Secondary Organic Aerosol Production from Local Emissions Dominates the Organic Aerosol Budget over Seoul, South Korea, during KORUS-AQ. *Atmos. Chem. Phys.* **2018**, *18* (24), 17769−17800.
(100) Aiken, A. C.; Salcedo, D.; Cubison, M. J.; Huffman, J. A.; DeCarlo, P. F.; Ulbrich, I. M.; Docherty, K. S.; Sueper, D.; Kimmel, J. R.; Worsnop, D. R.; et al. Mexico City Aerosol Analysis during MILAGRO Using High Resolution Aerosol Mass Spectrometry at the Urban Supersite (T0)−Part 1: Fine Particle Composition and Organic Source Apportionment. *Atmos. Chem. Phys.* **2009**, *9* (17), 6633−6653.
(101) Lee, T.; Sullivan, A. P.; Mack, L.; Jimenez, J. L.; Kreidenweis, S. M.; Onasch, T. B.; Worsnop, D. R.; Malm, W.; Wold, C. E.; Hao, W. M.; et al. Chemical Smoke Marker Emissions During Flaming and Smoldering Phases of Laboratory Open Burning of Wildland Fuels. *Aerosol Sci. Technol.* **2010**, *44* (9), i−v.
(102) Huffman, J. A.; Docherty, K. S.; Mohr, C.; Cubison, M. J.; Ulbrich, I. M.; Ziemann, P. J.; Onasch, T. B.; Jimenez, J. L. Chemically-Resolved Volatility Measurements of Organic Aerosol from Different Sources. *Environ. Sci. Technol.* **2009**, *43* (14), 5351−5357.
(103) Sullivan, A. P.; May, A. A.; Lee, T.; McMeeking, G. R.; Kreidenweis, S. M.; Akagi, S. K.; Yokelson, R. J.; Urbanski, S. P.; Collett, J. L., Jr. Airborne Characterization of Smoke Marker Ratios from Prescribed Burning. *Atmos. Chem. Phys.* **2014**, *14* (19), 10535−10545.
(104) Volkamer, R.; Jimenez, J. L.; San Martini, F.; Dzepina, K.; Zhang, Q.; Salcedo, D.; Molina, L. T.; Worsnop, D. R.; Molina, M. J. Secondary Organic Aerosol Formation from Anthropogenic Air Pollution: Rapid and Higher than Expected. *Geophys. Res. Lett.* **2006**, *33* (17), 4407.
(105) Jimenez, J. L.; Canagaratna, M. R.; Donahue, N. M.; Prevot, A. S. H.; Zhang, Q.; Kroll, J. H.; DeCarlo, P. F.; Allan, J. D.; Coe, H.; Ng, N. L.; et al. Evolution of Organic Aerosols in the Atmosphere. *Science* **2009**, *326* (5959), 1525−1529.
(106) Cappa, C. D.; Jimenez, J. L. Quantitative Estimates of the Volatility of Ambient Organic Aerosol. *Atmos. Chem. Phys.* **2010**, *10* (12), 5409−5424.
(107) Alfarra, M. R.; Coe, H.; Allan, J. D.; Bower, K. N.; Boudries, H.; Canagaratna, M. R.; Jimenez, J. L.; Jayne, J. T.; Garforth, A. A.; Li, S.-M.; et al. Characterization of Urban and Rural Organic Particulate in the Lower Fraser Valley Using Two Aerodyne Aerosol Mass Spectrometers. *Atmos. Environ.* **2004**, *38* (34), 5745−5758.
(108) Canagaratna, M. R.; Jimenez, J. L.; Kroll, J. H.; Chen, Q.; Kessler, S. H.; Massoli, P.; Hildebrandt Ruiz, L.; Fortner, E.; Williams, L. R.; Wilson, K. R.; et al. Elemental Ratio Measurements of Organic Compounds Using Aerosol Mass Spectrometry: Characterization, Improved Calibration, and Implications. *Atmos. Chem. Phys.* **2015**, *15* (1), 253−272.
(109) Aiken, A. C.; Decarlo, P. F.; Kroll, J. H.; Worsnop, D. R.; Huffman, J. A.; Docherty, K. S.; Ulbrich, I. M.; Mohr, C.; Kimmel, J. R.; Sueper, D.; et al. O/C and OM/OC Ratios of Primary, Secondary, and Ambient Organic Aerosols with High-Resolution Time-of-Flight Aerosol Mass Spectrometry. *Environ. Sci. Technol.* **2008**, *42* (12), 4478−4485.
(110) Hayes, P. L.; Carlton, A. G.; Baker, K. R.; Ahmadov, R.; Washenfelder, R. A.; Alvarez, S.; Rappenglück, B.; Gilman, J. B.; Kuster, W. C.; Gouw, J. A.; et al. Modeling the Formation and Aging of Secondary Organic Aerosols in Los Angeles during CalNex 2010. *Atmos. Chem. Phys.* **2015**, *15* (10), 5773−5801.
(111) DeCarlo, P. F.; Ulbrich, I. M.; Crounse, J.; Foy, B.; Dunlea, E. J.; Aiken, A. C.; Knapp, D.; Weinheimer, A. J.; Campos, T.; Wennberg, P. O.; et al. Investigation of the Sources and Processing of Organic Aerosol over the Central Mexican Plateau from Aircraft Measurements during MILAGRO. *Atmos. Chem. Phys.* **2010**, *10* (12), 5257−5280.
(112) Yokelson, R. J.; Griffith, D. W. T.; Ward, D. E. Open-Path Fourier Transform Infrared Studies of Large-Scale Laboratory Biomass Fires. *J. Geophys. Res. D: Atmos.* **1996**, *101* (D15), 21067−21080.
(113) Hennigan, C. J.; Miracolo, M. A.; Engelhart, G. J.; May, A. A.; Presto, A. A.; Lee, T.; Sullivan, A. P.; McMeeking, G. R.; Coe, H.; Wold, C. E.; et al. Chemical and Physical Transformations of Organic Aerosol from the Photo-Oxidation of Open Biomass Burning Emissions in an Environmental Chamber. *Atmos. Chem. Phys.* **2011**, *11* (15), 7669−7686.
(114) Ortega, A. M.; Day, D. A.; Cubison, M. J.; Brune, W. H.; Bon, D.; Gouw, J. A.; Jimenez, J. L. Secondary Organic Aerosol Formation

and Primary Organic Aerosol Oxidation from Biomass-Burning Smoke in a Flow Reactor during FLAME-3. *Atmos. Chem. Phys.* **2013**, *13* (22), 11551−11571.
(115) Tkacik, D. S.; Robinson, E. S.; Ahern, A.; Saleh, R.; Stockwell, C.; Veres, P.; Simpson, I. J.; Meinardi, S.; Blake, D. R.; Yokelson, R. J.; et al. A Dual-Chamber Method for Quantifying the Effects of Atmospheric Perturbations on Secondary Organic Aerosol Formation from Biomass Burning Emissions: Investigation of Biomass Burning SOA. *J. Geophys. Res. D: Atmos.* **2017**, *122* (11), 6043−6058.
(116) Ahern, A. T.; Robinson, E. S.; Tkacik, D. S.; Saleh, R.; Hatch, L. E.; Barsanti, K. C.; Stockwell, C. E.; Yokelson, R. J.; Presto, A. A.; Robinson, A. L.; et al. Production of Secondary Organic Aerosol During Aging of Biomass Burning Smoke From Fresh Fuels and Its Relationship to VOC Precursors. *J. Geophys. Res.: Atmos.* **2019**, *124* (6), 3583−3606.
(117) Weitkamp, E. A.; Sage, A. M.; Pierce, J. R.; Donahue, N. M.; Robinson, A. L. Organic Aerosol Formation from Photochemical Oxidation of Diesel Exhaust in a Smog Chamber. *Environ. Sci. Technol.* **2007**, *41* (20), 6969−6975.
(118) Krechmer, J. E.; Pagonis, D.; Ziemann, P. J.; Jimenez, J. L. Quantification of Gas-Wall Partitioning in Teflon Environmental Chambers Using Rapid Bursts of Low-Volatility Oxidized Species Generated in Situ. *Environ. Sci. Technol.* **2016**, *50* (11), 5757−5765.
(119) Bian, Q.; Jathar, S. H.; Kodros, J. K.; Barsanti, K. C.; Hatch, L. E.; May, A. A.; Kreidenweis, S. M.; Pierce, J. R. Secondary Organic Aerosol Formation in Biomass-Burning Plumes: Theoretical Analysis of Lab Studies and Ambient Plumes. *Atmos. Chem. Phys.* **2017**, *17* (8), 5459−5475.
(120) Yokelson, R. J.; Burling, I. R.; Gilman, J. B.; Warneke, C.; Stockwell, C. E.; Gouw, J.; Akagi, S. K.; Urbanski, S. P.; Veres, P.; Roberts, J. M.; et al. Coupling Field and Laboratory Measurements to Estimate the Emission Factors of Identified and Unidentified Trace Gases for Prescribed Fires. *Atmos. Chem. Phys.* **2013**, *13* (1), 89−116.
(121) Jiang, X.; Tsona, N. T.; Jia, L.; Liu, S.; Xu, Y.; Du, L. Secondary Organic Aerosol Formation from Photooxidation of Furan: Effects of NOx Level and Humidity. *Atmos. Chem. Phys. Discuss.* **2018**, *2018*, 1−27.
(122) Stefenelli, G.; Jiang, J.; Bertrand, A.; Bruns, E. A.; Pieber, S. M.; Baltensperger, U.; Marchand, N.; Aksoyoglu, S.; Prévôt, A. S. H.; Slowik, J. G.; et al. Secondary Organic Aerosol Formation from Smoldering and Flaming Combustion of Biomass: A Box Model Parametrization Based on Volatility Basis Set. *Atmos. Chem. Phys. Discuss.* **2019**, 1−41.
(123) Selimovic, V.; Yokelson, R. J.; Warneke, C.; Roberts, J. M.; Gouw, J.; Reardon, J.; Griffith, D. W. T. Aerosol Optical Properties and Trace Gas Emissions by PAX and OP-FTIR for Laboratory-Simulated Western US Wildfires during FIREX. *Atmos. Chem. Phys.* **2018**, *18* (4), 2929−2948.
(124) Jathar, S. H.; Gordon, T. D.; Hennigan, C. J.; Pye, H. O. T.; Pouliot, G.; Adams, P. J.; Donahue, N. M.; Robinson, A. L. Unspeciated Organic Emissions from Combustion Sources and Their Influence on the Secondary Organic Aerosol Budget in the United States. *Proc. Natl. Acad. Sci. U. S. A.* **2014**, *111* (29), 10473−10478.
(125) Stockwell, C. E.; Yokelson, R.; Kreidenweis, S. M.; Robinson, A. L.; DeMott, P. J.; Sullivan, R. C.; Reardon, J.; Ryan, K. C.; Griffith, D. W. T.; Stevens, L. Trace gas emissions from combustion of peat, crop residue, domestic biofuels, grasses, and other fuels: Configuration and Fourier transform infrared (FTIR) component of the Fourth Fire Lab at Missoula Experiment (FLAME-4). *Atmos. Chem. Phys.***2014**.*149727*
(126) Stockwell, C. E.; Veres, P. R.; Williams, J.; Yokelson, R. J. Characterization of Biomass Burning Emissions from Cooking Fires, Peat, Crop Residue, and Other Fuels with High-Resolution Proton-Transfer-Reaction Time-of-Flight Mass Spectrometry. *Atmos. Chem. Phys.* **2015**, *15* (2), 845−865.
(127) Sekimoto, K.; Koss, A. R.; Gilman, J. B.; Selimovic, V.; Coggon, M. M.; Zarzana, K. J.; Yuan, B.; Lerner, B. M.; Brown, S. S.; Warneke, C.; et al. High- and low-temperature pyrolysis profiles describe volatile organic compound emissions from western US wildfire fuels. *Atmos. Chem. Phys.* **2018**, *18* (13). 9263.
(128) Van der Werf, G. R.; Randerson, J. T.; Giglio, L.; Collatz, G. J.; Mu, M.; Kasibhatla, P. S.; Morton, D. C.; DeFries, R. S.; van Jin, Y.; van Leeuwen, T. T. Global Fire Emissions and the Contribution of Deforestation, Savanna, Forest, Agricultural, and Peat Fires (1997–2009). *Atmos. Chem. Phys.* **2010**, *10* (23), 11707−11735.
(129) Davies, G. M.; Kettridge, N.; Stoof, C. R.; Gray, A.; Ascoli, D.; Fernandes, P. M.; Marrs, R.; Allen, K. A.; Doerr, S. H.; Clay, G. D.; et al. The role of fire in UK peatland and moorland management: The need for informed, unbiased debate. *Philos. Trans. R. Soc., B* **2016**, *371* (1696). 20150342.
(130) Liu, X.; Huey, L. G.; Yokelson, R. J.; Selimovic, V.; Simpson, I. J.; Müller, M.; Jimenez, J. L.; Campuzano-Jost, P.; Beyersdorf, A. J.; Blake, D. R.; et al. Airborne Measurements of Western US Wildfire Emissions: Comparison with Prescribed Burning and Air Quality Implications. *J. Geophys. Res. D: Atmos.* **2017**, *122* (11), 6108−6129.
(131) Jolleys, M. D.; Coe, H.; McFiggans, G.; McMeeking, G. R.; Lee, T.; Kreidenweis, S. M.; Collett, J. L., Jr; Sullivan, A. P. Organic Aerosol Emission Ratios from the Laboratory Combustion of Biomass Fuels. *J. Geophys. Res. D: Atmos.* **2014**, *119* (22), 12−850.
(132) Finney, M. A.; Cohen, J. D.; Forthofer, J. M.; McAllister, S. S.; Gollner, M. J.; Gorham, D. J.; Saito, K.; Akafuah, N. K.; Adam, B. A.; English, J. D. Role of Buoyant Flame Dynamics in Wildfire Spread. *Proc. Natl. Acad. Sci. U. S. A.* **2015**, *112* (32), 9833−9838.
(133) Campbell, J.; Donato, D.; Azuma, D.; Law, B. Pyrogenic carbon emission from a large wildfire in Oregon, United States. *J. Geophys. Res., Biogeosci.* **2007**, *112* (G4).n/a
(134) Santín, C.; Doerr, S. H.; Preston, C. M.; González-Rodríguez, G. Pyrogenic Organic Matter Production from Wildfires: A Missing Sink in the Global Carbon Cycle. *Glob. Chang. Biol.* **2015**, *21* (4), 1621−1633.
(135) Smith, J. D.; Kroll, J. H.; Cappa, C. D.; Che, D. L.; Liu, C. L.; Ahmed, M.; Leone, S. R.; Worsnop, D. R.; Wilson, K. R. The Heterogeneous Reaction of Hydroxyl Radicals with Sub-Micron Squalane Particles: A Model System for Understanding the Oxidative Aging of Ambient Aerosols. *Atmos. Chem. Phys.* **2009**, *9* (9), 3209−3222.
(136) Kroll, J. H.; Donahue, N. M.; Jimenez, J. L.; Kessler, S. H.; Canagaratna, M. R.; Wilson, K. R.; Altieri, K. E.; Mazzoleni, L. R.; Wozniak, A. S.; Bluhm, H.; et al. Carbon Oxidation State as a Metric for Describing the Chemistry of Atmospheric Organic Aerosol. *Nat. Chem.* **2011**, *3* (2), 133−139.
(137) Andreae, M. O.; Merlet, P. Emission of Trace Gases and Aerosols from Biomass Burning. *Global Biogeochem. Cycles* **2001**, *15* (4), 955−966.
(138) Mebust, A. K.; Cohen, R. C. Observations of a Seasonal Cycle in NOx Emissions from Fires in African Woody Savannas. *Geophys. Res. Lett.* **2013**, *40*, 1451.
(139) Brown, S. S.; Dibb, J. E.; Stark, H.; Aldener, M.; Vozella, M.; Whitlow, S.; Williams, E. J.; Lerner, B. M.; Jakoubek, R.; Middlebrook, A. M.; et al. Nighttime Removal of NOx in the Summer Marine Boundary Layer. *Geophys. Res. Lett.* **2004**, *31* (7).n/a
(140) Pósfai, M.; Gelencsér, A.; Simonics, R.; Arató, K.; Li, J.; Hobbs, P. V.; Buseck, P. R. Atmospheric tar balls: Particles from biomass and biofuel burning. *J. Geophys. Res.* **2004**, *109* (D6). DOI: 10.1029/2003JD004169.
(141) Sedlacek, A. J., III; Buseck, P. R.; Adachi, K.; Onasch, T. B.; Springston, S. R.; Kleinman, L. Formation and Evolution of Tar Balls from Northwestern US Wildfires. *Atmos. Chem. Phys.* **2018**, *18* (15), 11289−11301.
(142) Eatough, D. J.; Eatough, N. L.; Pang, Y.; Sizemore, S.; Kirchstetter, T. W.; Novakov, T.; Hobbs, P. V. Semivolatile particulate organic material in southern Africa during SAFARI 2000. *J. Geophys. Res. D, Atmos.* **2003**, *108* (D13).n/a
(143) Grieshop, A. P.; Donahue, N. M.; Robinson, A. L. Laboratory Investigation of Photochemical Oxidation of Organic Aerosol from Wood Fires 2: Analysis of Aerosol Mass Spectrometer Data. *Atmos. Chem. Phys.* **2009**, *9* (6), 2227−2240.

DOI: 10.1021/acs.est.9b02588
Environ. Sci. Technol. 2019, 53, 10007−10022

(144) May, A. A.; Levin, E. J. T.; Hennigan, C. J.; Riipinen, I.; Lee, T.; Collett, J. L.; Jimenez, J. L.; Kreidenweis, S. M.; Robinson, A. L. Gas-particle partitioning of primary organic aerosol emissions: 3. Biomass burning. *J. Geophys. Res. D, Atmos.* **2013**, *118* (19).11,327
(145) Hodshire, A. L.; Bian, Q.; Ramnarine, E.; Lonsdale, C. R.; Alvarado, M. J.; Kreidenweis, S. M.; Jathar, S. H.; Pierce, J. R. More Than Emissions and Chemistry: Fire Size, Dilution, and Background Aerosol Also Greatly Influence Near-Field Biomass Burning Aerosol Aging. *J. Geophys. Res.: Atmos.* **2019**, *30*, 1783.
(146) Akherati, A.; Cappa, C. D.; Kleeman, M. J.; Docherty, K. S.; Jimenez, J. L.; Griffith, S. M.; Dusanter, S.; Stevens, P. S.; Jathar, S. H. Simulating Secondary Organic Aerosol in a Regional Air Quality Model Using the Statistical Oxidation Model–Part 3: Assessing the Influence of Semi-Volatile and Intermediate-Volatility Organic Compounds and NO X. *Atmos. Chem. Phys.* **2019**, *19* (7), 4561−4594.
(147) Donahue, N. M.; Robinson, A. L.; Pandis, S. N. Atmospheric Organic Particulate Matter: From Smoke to Secondary Organic Aerosol. *Atmos. Environ.* **2009**, *43* (1), 94−106.
(148) Barsanti, K. C.; Pankow, J. F. Thermodynamics of the Formation of Atmospheric Organic Particulate Matter by Accretion reactions—Part 1: Aldehydes and Ketones. *Atmos. Environ.* **2004**, *38* (26), 4371−4382.
(149) Andela, N.; Morton, D. C.; Giglio, L.; Paugam, R.; Chen, Y.; Hantson, S.; Werf, G. R.; Randerson, J. T. The Global Fire Atlas of Individual Fire Size, Duration, Speed and Direction. *Earth System Science Data* **2019**, *11* (2), 529−552.
(150) Liousse, C.; Devaux, C.; Dulac, F.; Cachier, H. Aging of Savanna Biomass Burning Aerosols: Consequences on Their Optical Properties. *J. Atmos. Chem.* **1995**, *22* (1), 1−17.
(151) Colarco, P. R.; Schoeberl, M. R.; Doddridge, B. G.; Marufu, L. T.; Torres, O.; Welton, E. J. Transport of smoke from canadian forest fires to the surface near Washington, DC: Injection height, entrainment, and optical properties. *J. Geophys. Res. D, Atmos.* **2004**, *109* (D6).n/a
(152) Baylon, P.; Jaffe, D. A.; Hall, S. R.; Ullmann, K.; Alvarado, M. J.; Lefer, B. L. Impact of Biomass Burning Plumes on Photolysis Rates and Ozone Formation at the Mount Bachelor Observatory. *J. Geophys. Res. D: Atmos.* **2018**, *123* (4), 2272−2284.
(153) Martin, S. T.; Artaxo, P.; Machado, L. A. T. Introduction: Observations and Modeling of the Green Ocean Amazon (GoAmazon2014/5). *Atmos. Chem. Phys.* **2016**. DOI: 10.5194/acp-16-4785-2016
(154) Lambe, A. T.; Ahern, A. T.; Williams, L. R.; Slowik, J. G.; Wong, J. P. S.; Abbatt, J. P. D.; Brune, W. H.; Ng, N. L.; Wright, J. P.; Croasdale, D. R.; et al. Characterization of Aerosol Photooxidation Flow Reactors: Heterogeneous Oxidation, Secondary Organic Aerosol Formation and Cloud Condensation Nuclei Activity Measurements. *Atmos. Meas. Tech.* **2011**, *4* (3), 445−461.
(155) Palm, B. B.; Campuzano-Jost, P.; Ortega, A. M.; Day, D. A.; Kaser, L.; Jud, W.; Karl, T.; Hansel, A.; Hunter, J. F.; Cross, E. S.; et al. In Situ Secondary Organic Aerosol Formation from Ambient Pine Forest Air Using an Oxidation Flow Reactor. *Atmos. Chem. Phys.* **2016**, *16* (5), 2943−2970.
(156) Eluri, S.; Cappa, C. D.; Friedman, B.; Farmer, D. K.; Jathar, S. H. Modeling the Formation and Composition of Secondary Organic Aerosol from Diesel Exhaust Using Parameterized and Semi-Explicit Chemistry and Thermodynamic Models. *Atmos. Chem. Phys.* **2018**, *18* (19), 13813−13838.
(157) Pratap, V.; Bian, Q.; Kiran, S. A.; Hopke, P. K.; Pierce, J. R.; Nakao, S. Investigation of Levoglucosan Decay in Wood Smoke Smog-Chamber Experiments: The Importance of Aerosol Loading, Temperature, and Vapor Wall Losses in Interpreting Results. *Atmos. Environ.* **2019**, *199*, 224−232.
(158) Bian, Q.; May, A. A.; Kreidenweis, S. M.; Pierce, J. R. Investigation of Particle and Vapor Wall-Loss Effects on Controlled Wood-Smoke Smog-Chamber Experiments. *Atmos. Chem. Phys.* **2015**, *15* (19), 11027−11045.
(159) Pagonis, D.; Krechmer, J. E.; Gouw, J.; Jimenez, J. L.; Ziemann, P. J. Effects of Gas−wall Partitioning in Teflon Tubing and Instrumentation on Time-Resolved Measurements of Gas-Phase Organic Compounds. *Atmos. Meas. Tech.* **2017**, *10* (12), 4687−4696.
(160) Deming, B. L.; Pagonis, D.; Liu, X.; Day, D. A.; Talukdar, R.; Krechmer, J. E.; Gouw, J. A. de; Jimenez, J. L.; Ziemann, P. J. Measurements of Delays of Gas-Phase Compounds in a Wide Variety of Tubing Materials due to Gas−wall Interactions. *Atmos. Meas. Tech.* **2019**, *12* (6), 3453−3461.
(161) Liu, X.; Deming, B.; Pagonis, D.; Day, D. A.; Palm, B. B.; Talukdar, R.; Roberts, J. M.; Veres, P. R.; Krechmer, J. E.; Thornton, J. A.; et al. Effects of Gas−wall Interactions on Measurements of Semivolatile Compounds and Small Polar Molecules. *Atmos. Meas. Tech.* **2019**, *12* (6), 3137−3149.
(162) Riipinen, I.; Pierce, J. R.; Donahue, N. M.; Pandis, S. N. Equilibration Time Scales of Organic Aerosol inside Thermodenuders: Evaporation Kinetics versus Thermodynamics. *Atmos. Environ.* **2010**, *44* (5), 597−607.
(163) Lopez-Hilfiker, F. D.; Pospisilova, V.; Huang, W.; Kalberer, M.; Stefenelli, G.; Thornton, J. A.; Baltensperger, U.; Prevot, A. S. H.; Slowik, J. G. An Extractive Electrospray Ionization Time-of-Flight Mass Spectrometer (EESI-TOF) for Online Measurement of Atmospheric Aerosol Particles. *Atmospheric Measurement Techniques Discussions.* **2019**, 1.
(164) Hodshire, A. L.; Palm, B. B.; Alexander, M. L.; Bian, Q.; Campuzano-Jost, P.; Cross, E. S.; Day, D. A.; Sá, S. S.; Guenther, A. B.; Hansel, A.; et al. Constraining Nucleation, Condensation, and Chemistry in Oxidation Flow Reactors Using Size-Distribution Measurements and Aerosol Microphysical Modeling. *Atmos. Chem. Phys.* **2018**, *18* (16), 12433−12460.

NOTE ADDED AFTER ASAP PUBLICATION

This paper published ASAP on August 12, 2019 with an incorrect version of Figure 1. The corrected version of the paper reposted on August 13, 2019.

DOI: 10.1021/acs.est.9b02588
Environ. Sci. Technol. 2019, 53, 10007−10022